

Synthesis And Characterization Of Fe Doped $\text{Bi}_2\text{Sr}_2\text{CaCu}_2\text{O}_8$

A thesis submitted in partial fulfillment for the award of degree in

**Master of Science
in
Physics**
By

**Amrita Singh
Roll No. - 411PH2086**

Under the guidance of

**Dr. Prakash Nath Vishwakarma
Department of Physics**



**National Institute Of Technology, Rourkela
Rourkela- 769008, Odisha, India
May- 2013**

Declaration

I hereby declare that the project work entitled “**Synthesis And Characterization Of Fe Doped $\text{Bi}_2\text{Sr}_2\text{Ca}_1\text{Cu}_2\text{O}_8$** ” submitted to National Institute of Technology, Rourkela, is the record of an original work done by me under the guidance of Dr. Prakash Nath Vishwakarma, Assistant professor of NIT, Rourkela, and this project work has not performed the basis for the award of any degree or diploma/associate-ship/fellowship and similar project if any.

Amrita Singh

Roll No.- 411PH2086

NIT, Rourkela

Acknowledgements

I owe a debt of gratitude to Prof. Sunil Kumar Sarangi, The Director ,NIT, Rourkela for his vision and foresight of this One year Project which has immensely helped all of us to get a flavor and feel of research.

I'd also like to take this opportunity to express appreciation towards our Guide Prof. P.N Vishwakarma for his continuous advice, support. His valuable guidance and suggestions helped me a lot to carry out this project.

It's also my duty to record my utmost gratefulness to Ph.D. Scholars Miss Jashashree Ray and Mr.Achyuta Ku.Biswal for their guidance and insights throughout this period.

I am also very thankful to my labmate Sikha Kanungo and all my batchmates for their support and affection.

Last but not the least my parents, in-laws, husband and all my family members for their support, blessings, encouragement and everything.

CERTIFICATE

This is to certify that the thesis entitled “**Synthesis And Characterization Of Fe Doped $\text{Bi}_2\text{Sr}_2\text{Ca}_1\text{Cu}_2\text{O}_8$** ” submitted by **Amrita Singh** in partial fulfilment of the requirements for the award of degree of Master of Science in Physics at National Institute of Technology, Rourkela is an authentic work carried out by her under my supervision. To the best of my knowledge, the work done in this thesis has not been submitted by any other university/ Institute for the award of any degree or diploma.

Technology

Dr. Prakash Nath Vishwakarma
Assistant Professor
National Institute of

Rourkela

Date:

Table Of Content

- List of Figures
- Abstract

Chapter 1: Superconductivity, An overview

- 1.1 Introduction
- 1.2 History of Superconductors
- 1.3 Superconductors
- 1.4 Superconductor Theories
- 1.5 High Temperature Superconductor
- 1.6 Properties of High Temperature Superconductor
- 1.7 Josephson Junction
- 1.8 Types of Superconductor
- 1.9 Flux Quantization
- 1.10 Role of transition metal doping in BSCCO 2212 phase
- 1.11 Bi- base Superconductor
- 1.12 Crystal Structure of BSCCO 2212
- 1.13 Literature Survey

Chapter 2: Sample Preparation

- 2.1 Synthesis Of BSCCO-2212
- 2.2 Synthesis of Fe doped BSCCO with different concentration
- 2.3 Characterization Techniques

Chapter 3: Result and Discussion

3.1 XRD Analysis

3.2 SEM Analysis

3.3 Resistivity VS Temperature Analysis

Chapter 4:

- Conclusion

- References

List of Figures

1.2 Chronological order of discovery of superconductor

1.3(a) Sudden drop in resistivity $\rho = 0$ at a temperature T_c , compared to a nonsuperconducting behavior.

1.3 (b) Corresponding drop in susceptibility to the ideal diamagnetic value of $\chi = -1$ below T_c . The onset of the diamagnetic response corresponds quite closely to the point where $\rho \rightarrow 0$ on the temperature axis. The figure also indicates that χ is positive but quite small above T_c .

1.4(a) Meissner Effect

1.4(d) BCS Theory

1.6.3 Superconducting Critical Surface

1.8 Types Of Superconductor

1.9 Magnetic flux lines in type II superconductor

1.12 Crystal structure of BSCCO

2.3.1 Systematic XRD system

2.3.2 Scanning Electron Microscope

2.3.3(a) Four Probe measurement technique

2.3.3(b) Van der pauw method

3.1 X-Ray Diffraction Pattern of BSCCO, 1%, 3% & 5% Fe doped

3.2 SEM micrographs of parent and Fe doped in BSCCO 2212

3.3(a) Temperature Variation of normalized resistivity ρ/ρ_{273} for BSCCO and 1%, 3%, 5% Fe doped

3.3(b) Resistivity V_s Temperature graph of BSCCO, 1% Fe, 3% Fe & 5% Fe

3.4(a) V-I characteristic of parent BSCCO, 1% Fe, 3% Fe & 5% Fe

3.4(c) Variation of critical current density J_c as a function of temperature for BSCCO, 1% Fe, 3% Fe & 5% Fe

Abstract

$\text{Bi}_2\text{Sr}_2\text{CaCu}_2\text{O}_8$ (BSCCO) was prepared by solid state route method. Our aim is to dope BSCCO with a magnetic material such as Fe to enhance its current density. Samples were prepared by conventional solid state reaction method followed by sintering at 880°C . Critical temperatures of the samples were determined by resistivity temperature measurements using four probe technique at liquid nitrogen temperatures. T_c values for the samples were in the range ($T_{\text{conset}} \sim 78 - 60\text{K}$). XRD analyses were done and lattice parameters of the samples were determined by indexing the diffraction peaks. Surface of the samples was studied by scanning electron microscope (SEM) micrographs at a magnification of X1000.

Chapter – I

Superconductivity, an Overview

1.1 Introduction

Superconductivity was first observed by Dutch physicist Heike Kammerlingh Onnes, while studying the resistivity of mercury at cryogenic temperatures using liquid helium. He was also first to liquefy Helium (which boils at 4.2K at standard pressure). So for the first time it became possible to achieve such a low temperature to achieve and witness superconductivity in any elements. After this discovery several other materials like lead, niobium nitride also showed superconductivity. While in superconducting state, these materials have the ability to transport large DC currents with no measurable resistive losses. For this the superconductor must be kept below three critical parameters, critical temperature(T_c), critical field(H_c), and critical density(J_c).

So wires made of superconducting materials, can be used for power transmission at high densities without any loss. In medical, it finds its uses in MRI, as superconducting magnet. Some other applications are in research laboratories, as particle accelerators, high field magnets, SQUIDs.

Before mid-80's its application was limited due to its cost associated to maintain such low temperature. Prospects for developing power applications rose with the discovery of high temperature superconductor (HTS) materials having critical temperatures higher than the boiling point of liquid nitrogen (77K).

1.2 Some milestones in the history of superconductors

- In 1911, K. Onnes discovered superconductivity while studying the resistivity of solid mercury at cryogenic temperature using Helium as refrigerant. He was awarded the Nobel prize for this discovery.
- In 1913, lead was found to superconduct at 7K and in 1941 niobium nitride was found to superconduct at 16K.
- In 1933, the phenomenon known as Meissner effect was discovered by Meissner and Ochsenfeld while studying superconductivity.
- In 1950 in order to understand the macroscopic properties of superconductor, Landau and Ginzburg put forward a theory known as Ginzburg-Landau based on Schrödinger wave

equation.

- In the same year 1950, Maxwell and Reynolds *et.al.* found the dependence of critical temperature on isotopic mass of the constituent element.
- The complete microscopic properties of superconductor were explained by Bardeen, Cooper and Schrieffer in 1957 by a theory known as BCS theory.
- In 1962, Josephson junction was discovered by Brian David Josephson.
- In 1986, Bednorz and Muller discovered a completely new class of superconductivity (also called cuprate based superconductors) in LaCuO₄ (T_c = 33K) based compound. This was the beginning of oxide based superconductors also called high T_c superconductors.

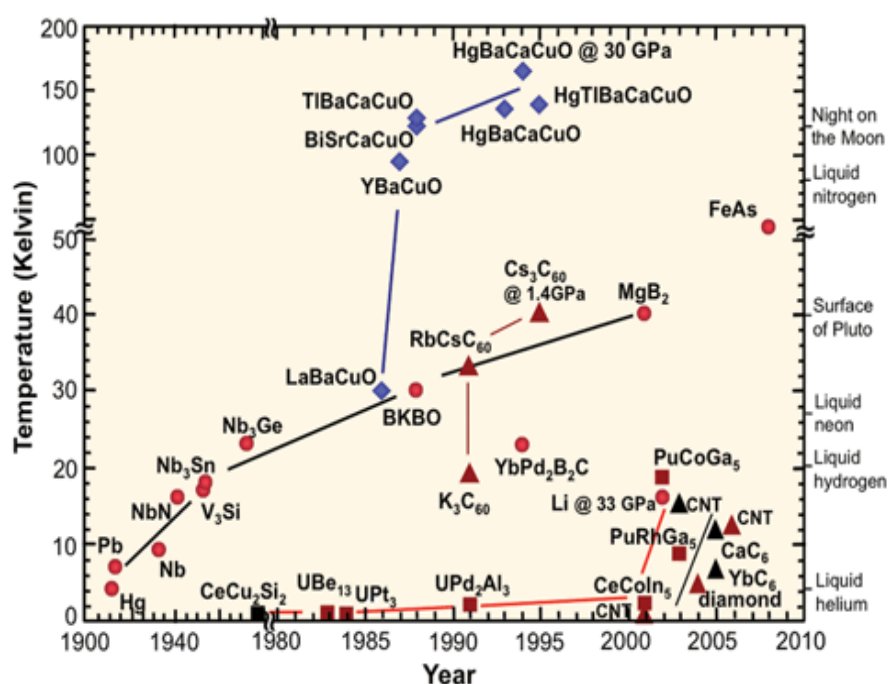


Fig:1.2 Chronological order of discovery of superconductor

Cuprate superconductor differs in many ways from the conventional superconductors.

They are layered compound, with structure either tetragonal or orthorhombic, and contain Cu-O plane with the formula CuO₂ lying normal to c-direction. These planes contain mobile charge carriers and are thought to be the seat of superconductivity. The carriers are localized in the plane and this makes weak contacts with the plane. So cuprates have anisotropic properties in both the normal and superconducting state. (ii) Their carrier density is relatively low compared with what is found in semi metals such as Bismuth. This means that the carriers are less heavily screened than they are in ordinary

metals and makes the Coulomb repulsion between them more important. It also increases the penetration depth ' λ '.

1.3 Superconductors

Superconductors are material which show zero electrical resistance and expulsion of magnetic fields when cooled below a certain temperature, called critical or transition temperature. Above this temperature the material becomes normal. Two important properties associated with the superconductivity are:

- (i) The transition from finite resistivity, ρ_n in the normal state above a superconducting transition temperature T_c to $\rho = 0$, i.e perfect dc conductivity, $\sigma = \infty$, below T_c .
- (ii) The simultaneous change of magnetic susceptibility χ from a small positive paramagnetic value above T_c to $\chi = -1$, i.e perfect diamagnetic below T_c .

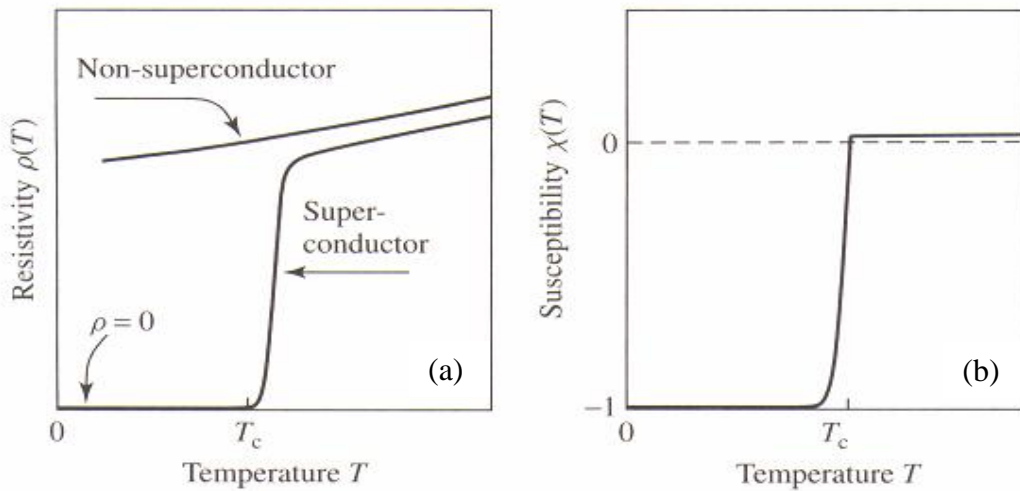


Fig 1.3. (a) shows a sudden drop in resistivity $\rho = 0$ at a temperature T_c , compared to a non superconducting behavior. (b) shows the corresponding drop in susceptibility to the ideal diamagnetic value of $\chi = -1$ below T_c . The onset of the diamagnetic response corresponds quite closely to the point where $\rho \rightarrow 0$ on the temperature axis. The figure also indicates that χ is positive but quite small above T_c .

1.4 Superconductor Theories

(a) Meissner Effect

When a superconductor is placed in a weak external magnetic field H , the field penetrates for only a short distance λ , called the London penetration depth, after which it decays rapidly to zero. This is called the Meissner effect and is one of the defining characteristics of superconductor. For most of the superconductor London penetration depth is of the order of 100nm. The Meissner effect is sometimes confused with the kind of diamagnetism one would expect in a perfect electrical conductor: according to Lenz's law, when a changing magnetic field is applied to a conductor, it will induce an electrical current in the conductor that creates an opposing magnetic field. In a perfect conductor, an arbitrarily large current can be induced, and the resulting magnetic field exactly cancels the applied field.

The Meissner effect was explained by London and London, who showed that the electromagnetic free energy in a superconductor is minimized provided

$$\Delta^2 H = H / \lambda^2,$$

where H is the magnetic field and λ is the London penetration depth. This equation, which is known as the London equation, predicts that the magnetic field in a superconductor decays exponentially from whatever value it possesses at the surface.

The Meissner effect breaks down when the applied magnetic field is too large.

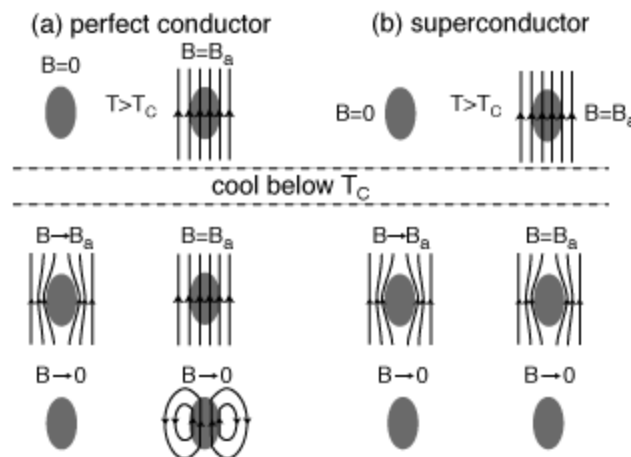


Fig: 1.4(a) Meissner Effect

(b) London Theory

In superconductor we assume that the current flows without dissipation and has the form

$$\mathbf{j}_s = n_s e \mathbf{v}_s$$

where the velocity of superconducting electrons is $\mathbf{v}_s = \mathbf{j}_s / n_s e$ where n_s is their density, now according to London Equation being non-dissipative this current contributes to the kinetic energy of superconducting electrons. The total free energy is a sum of the kinetic energy of superconducting electrons and the magnetic energy.

$$F = \frac{n_s v_s^2}{2} + \frac{h^2}{8\pi} dV = \frac{m j_s^2}{2 n_s e^2} + \frac{h^2}{8\pi} dV$$

Here h is the “microscopic” magnetic field. Its average over large area in the sample gives the magnetic induction B . Using the Maxwell equation

$$\mathbf{j}_s = (c/4\pi) \text{curl } \mathbf{h}$$

(c) Ginzburg-Landau Theory

The rich phenomenology of the superconducting state could be quantitatively described by the GL theory, without knowledge of the underlying microscopic mechanism based on the BCS theory. It uses the quantum mechanics to predict the effect of magnetic field. The first assumption of Ginzburg-Landau theory is that the behaviour of superconducting electron can be described by an effective wave function “ ψ ”, so that $|\psi(\mathbf{r})|^2$ represents the local density of superconducting electrons, $n_s(\mathbf{r})$. It is based on the idea that the superconducting transition is one of the second order phase transition. The amplitude ψ is zero in the normal phase above a superconducting transition temperature T_c , and is finite in the superconducting phase below T_c . In the presence of an external magnetic field, the order parameter has a spatial variation. When the spatial variation of the order parameter is taken into account, the free energy of the system can be expressed in terms of the order parameter ψ and its spatial derivative of ψ . In general this is valid in the vicinity of T_c (for $T < T_c$), where the amplitude ψ is small and the length scale for spatial variation is long.

The order parameter ψ is considered as a kind of a wave function for a particle of charge q^* and mass m^* . The macroscopic properties of superconductors can be explained by this theory. The superconductors are classed in two types: type I and type II superconductors. The Ginzburg-Landau parameter κ is the ratio of λ to ζ , where λ is the magnetic-field penetration depth and ζ is the coherence length of the superconducting phase. Ginzberg and Landau characterized type-I superconductors as those having $\kappa < 1/2$ and type-II superconductors having $\kappa > 1/2$.

(i) Penetration Depth

When a superconductor is placed in a weak external magnetic field H , the field penetrates for only a short distance λ , called the penetration depth, after which it decays rapidly to zero. It decreases monotonically with increasing temperature and rapidly drops to zero near the critical temperature. For most superconductors, the penetration depth is of the order of a hundred of nm.

(ii) Coherence Length

This length is a measure of the typical size of the Cooper pairs. It can also be taken as the minimum thickness of the interface between superconducting and normal regions. Coherence length is temperature dependent, being inversely proportional to the temperature difference from the critical value. Typical values are around 5 nm for type II superconductors and considerably larger for type I.

(d) BCS Theory

In order to explain the superconductivity three physicists Bardeen, Cooper and Schrieffer in 1957 put forward a theory for the quantum explanation of superconductivity and the properties exhibited by it. According to classical theory resistance in metal is due to collision between the free electrons and the crystal's lattice vibrations, known as phonon. In addition, part of the resistance is due to scattering of electrons from impurities or defects in the conductor. The main feature of this theory is that the two electrons in the superconductor are able to form a bound pair called a Cooper Pair because the lattice vibrations almost seizes at low temperature and they force the electrons to pair up into teams that could pass all of the obstacles which caused resistance in the conductor.

According to this theory when an electron passes through the positively charged ions in the lattice of superconductor, the lattice get distorts. This in turn causes phonons to be emitted which form a trough of positive charges around the electron. Figure 1.4(d) illustrates a wave of lattice distortion due to attraction to a moving electron.

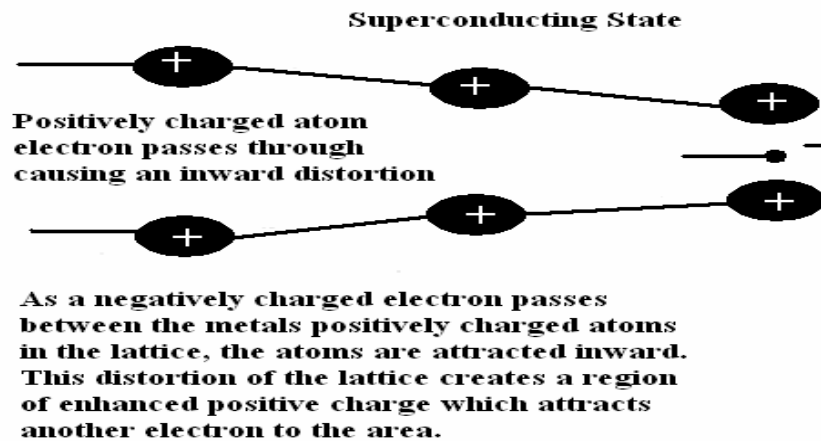


Fig:1.4(d) BCS Theory

Before the electron passes by and before the lattice springs back to its normal position, a second electron is drawn into the trough. It is through this process that two electrons, which should repel one another, link up. The forces exerted by the phonons overcome the electrons natural repulsion. The electron pairs are coherent with one another as they pass through the conductor in unison. The electrons are screened by the phonons and are separated by some distance. When one of the electrons that make up a Cooper pair and passes close to an ion in the crystal lattice, the attraction between the negative electron and the positive ion cause a vibration to pass from ion to ion until the other electron of the pair absorbs the vibration. The net effect is that the electron has emitted a phonon and the other electron has absorbed the phonon. It is this exchange that keeps the Cooper pairs together. It is important to understand, however, that the pairs are constantly breaking and reforming. Because electrons are indistinguishable particles, it is easier to think of them as permanently paired. Figure 1.4(d) illustrates how two electrons, called Cooper pairs, become locked together. Each electron in the solid is attracted to every other electron forming a large network of interactions. When the atoms of the lattice oscillate as positive and negative regions, the electron pair is alternatively pulled together and pushed apart without a collision. Here there is no collision with the lattice so, a small amount of energy is needed to destroy the superconducting state and make it normal. This energy is called energy gap.

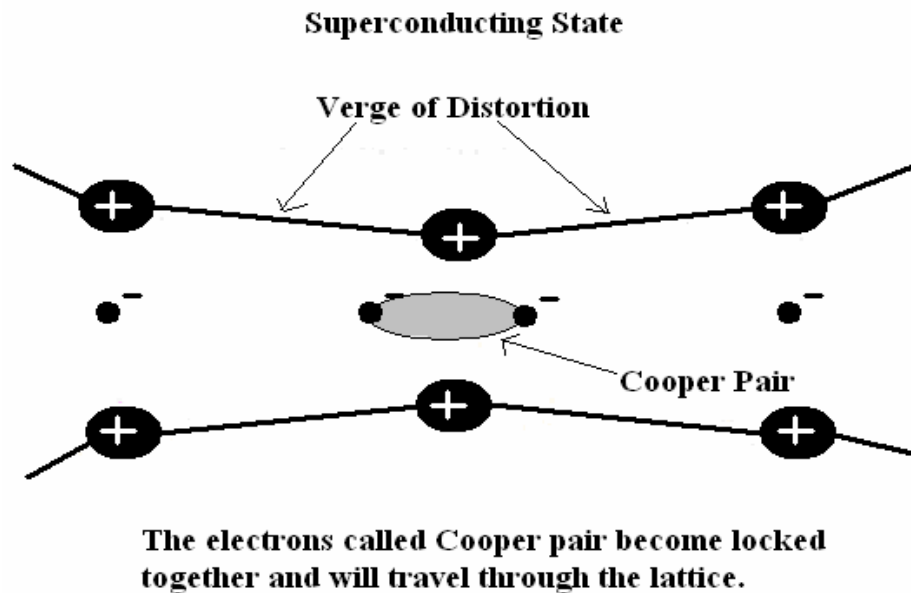


Fig:1.4(d) BCS Theory

1.5 High Temperature Superconductor

Nevertheless it has been a dream for the scientists working in the field of superconductivity to find a material that become superconductor at room temperature. In 1986 Bednorz and Muller found that in Ba- doped LaCuO_3 the temperature dependence of conductivity in the transition region from the normal state to the superconducting state changes with the current density and this pointed out the possibility of high temperature superconductor. In 1987, Chu and others found a new type of superconducting material $\text{YBa}_2\text{Cu}_3\text{O}_7$ with a critical temperature above 90K. So far the highest critical temperature of 135K has been achieved in Hg-based cuprate.

In $\text{YBa}_2\text{Cu}_3\text{O}_7$ conduction mostly occurs in the planes containing the copper oxide. It has been found that the critical temperature is very sensitive to the average number of oxygen atoms present, which can vary. For this reason the formula for 1-2-3 superconductor is sometimes given as $\text{YBa}_2\text{Cu}_3\text{O}_{7-\delta}$ where δ is a number between 0 and 1. The nominal distance between cooper pairs (coherence length) in these superconductors can be as short as one or two atomic spacing. As a result, the coulomb repulsion force will generally dominate at these distances causing electrons to be repelled rather than coupled. For this reason, it is widely accepted that Cooper pairs, in these materials, are not caused by a lattice deformation, but may be associated with the type of magnetism present (known as antiferromagnetism) in the copper oxide layers. So high- T_c superconductors cannot be explained by the BCS theory since

that mainly deals with a lattice deformation mediating the coupling of electron pairs. The research still continues to find the actual mechanism responsible for superconductivity in these material as there are various kind of interactions in such complicated system electron-phonon interactions, spin-spin interactions, charge density wave, spin density waves as it will take a long time to explain these phenomena.

1.6 Properties of High Temperature Superconductors

1.6.1 Critical temperature (T_c)

Superconducting metals and alloys have characteristic transition temperatures from normal conductors to superconductors called critical Temperature (T_c). Below the superconducting transition temperature, the resistivity of a material is exactly zero. As long as a superconductor is cooled below T_c , the Cooper pairs stay intact, due to the reduced molecular motion. As the superconductor gains heat energy the vibrations in the lattice become more violent and break the pairs. As they break, superconductivity diminishes. Superconductors made from different materials have different T_c values.

1.6.2 Critical Current Density (J_c)

If too much current is passed through a superconductor, it will revert to the normal state even though it may be below its transition temperature. The viability of high temperature superconductor depends on the size of the current density, they are able to support in high magnetic field.

1.6.3 Critical magnetic field(H_c)

The maximum value for the magnetic field at which the material remains in the superconducting state even below its T_c is known as the critical magnetic field (H_c). When a superconductor is cooled below its transition temperature (T_c) and applied magnetic field is increased gradually above certain magnetic field (H_c) the superconductivity is lost. It was found that in addition to a critical temperature, both current density and applied magnetic field have to be kept below their respective critical values (J_c and H_c) to maintain the superconducting state. Figure below illustrates the superconducting state as a region beneath a shaded 'critical surface' defined by the three critical parameters, J_c , H_c , and T_c .

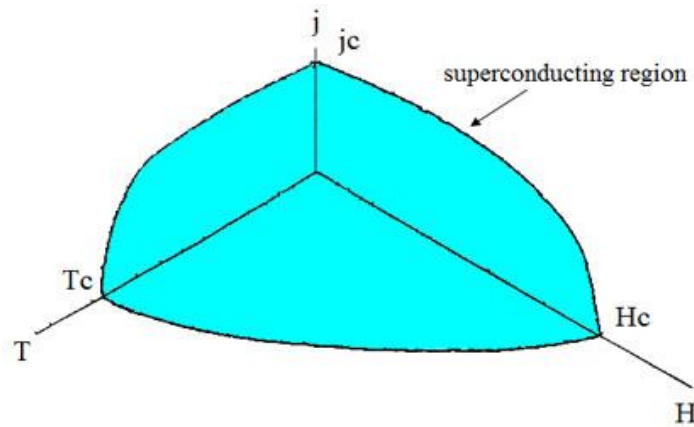


Fig:1.6.3 Superconducting critical surface

1.7 Josephson Junction

A Josephson junction consists of two superconductors separated by a thin insulating barrier. Pairs of superconducting electrons will tunnel through the barrier. As long as the current is below the critical current for the junction, there will be zero resistance and no voltage drop across the junction. Since then, this superconductor-insulator-superconductor sandwich has been called a “Josephson junction”. Such insulating layers act as a weak link between the superconductors.

1.8 Types of superconductors

High magnetic fields destroy superconductivity and restore the normal conducting state. Depending on this, superconductors have been classified into two types;

Type I Superconductor

Type I superconductors mainly comprised of metals and metalloids that show some conductivity at room temperature they require very low temperature to slow down their molecular vibrations and to support electron flow in accordance to BCS theory. It is characterized as “Soft Superconductor” which exclude the magnetic field until the superconductivity is destroyed suddenly, and then the field penetrates completely. They exhibit sharp transition to superconducting state.

Type II Superconductor

Type II superconductors are those superconductors which lose their superconductivity gradually but not easily or abruptly when placed in the external magnetic field. As can be seen in Fig:1.8 intensity of magnetization (M) versus applied magnetic field (H), when the type II superconductor is placed in the magnetic field, it gradually loses its superconductivity. Type II superconductors start to lose their superconductivity at lower critical magnetic field (H_{c1}) and completely lose their superconductivity at upper critical magnetic field (H_{c2}). The state between the lower critical magnetic field (H_{c1}) and upper

critical magnetic field (H_{c2}) is known as vortex state or intermediate state. These are also known as “Hard Superconductor” because they lose their superconductivity gradually.

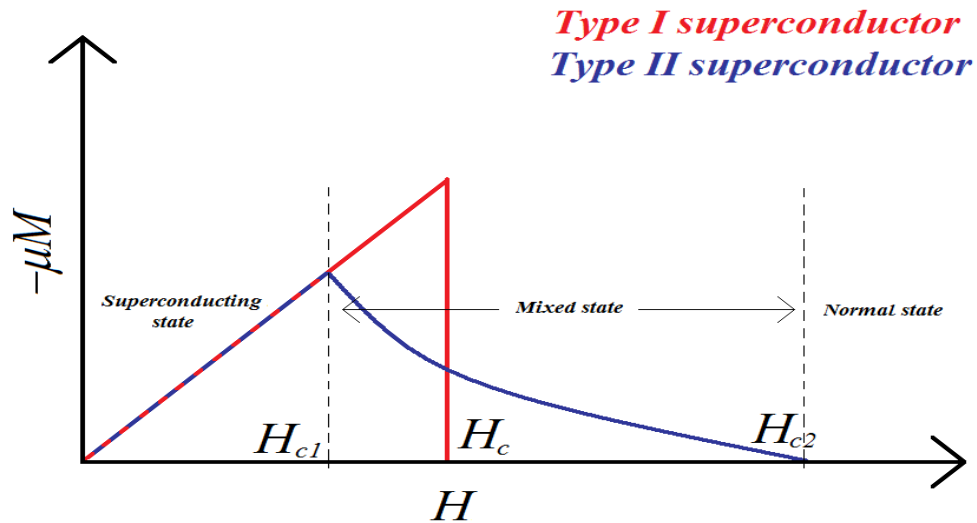


Fig: 1.8 Types of superconductor

1.9 Flux Quantization

Magnetic flux penetrates into a type II superconductor in the form of flux lines or vortices. Flux quantization is a quantum phenomenon in which the magnetic field is quantized in the unit of $\frac{h}{2e}$ also known as flux quanta, fluxoids, vortices. In type I superconductor below a critical field H_{c1} , all magnetic flux is expelled according to the Meissner effect and perfect diamagnetism is observed, but in type II superconductor flux penetrates and discrete unit up to a second critical field value, H_{c2} .

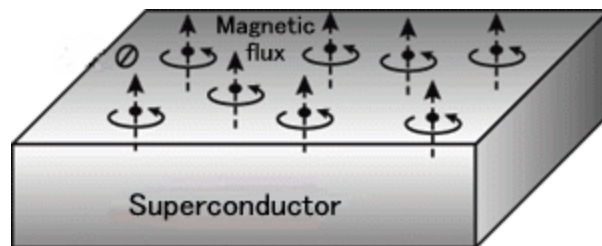


Fig: 1.9 Magnetic flux lines in type II superconductor

1.9.1 Flux Creep and Pinning

In high-T_c superconductors (HTSCs), a perfect superconducting state with a total expulsion of magnetic flux exists up to a lower critical field H_{c1}. At fields larger than the upper critical field H_{c2}, the magnetic fields penetrate the HTSC completely, and the material becomes normal.

HTSCs in applied magnetic fields of strength higher than H_{c1} and smaller than H_{c2} are known to be in the mixed state, where magnetic field penetrates the superconductors in the form of quantized magnetic vortices. When a transport current density, J is applied to HTSC in the mixed state it will produce a Lorentz force, F_L on the vortices trying to move them. The Lorentz force is given by;

$$F_L = 1/c \, J * \phi_0$$

Where ϕ_0 is the quantized magnetic flux per vortex i.e. $\phi_0 = h/2e = 2.0678 \times 10^{-7} \text{ G-cm}^2$

J- Transport current density and B is the applied magnetic field.

This Lorentz force tends to move the vortices transverse to both J and ϕ_0 . If the vortices move with velocity v they will induce an electric field, $E = -1/cB * v$ parallel to J, causing power to be dissipated. And an effective resistance will appear in the superconductor. If the vortices can be pinned and prevented from moving, no resistance will appear. Vortex pinning results from spatial inhomogeneities of the material which produces local reductions of the free energy of a flux line, thus attracting and holding vortices to these locations.

Unfortunately, the pinning of vortices in HTSCs is fairly weak, especially at high temperatures. The vortices can be effectively pinned by any structural inhomogeneities of the material. The effect of 3d magnetic elements (Fe, Co, Ni) and the nonmagnetic (Zn) doping in the Cu position of Bi-based superconducting materials have been extensively investigated. It was reported that the superconducting properties of these materials decrease with increase of the amount of doping regardless of the magnetic nature of the dopants, and the suppression of superconductivity was concluded to be due only to local disorder induced by the amount of doping.

1.10 Role of transition metal doping in BSCCO 2212 phase

HTSCs comprises a collection of tiny, randomly oriented anisotropic grains which are connected by weak links, and other impurity phases and defects. These types of granular networks are having considerably lower values of flux pinning and large critical current J_c anisotropy which lead to a poor performance in high applied magnetic fields and high temperatures. The method of systematic creation of point defects in the CuO₂ planes of the high-temperatures superconductors by replacing the Cu atoms by other 3d elements is a useful tool for probing parameters essential for the superconductivity. The Cu ions site are chosen for doping because of two reasons: (i) they constitute the essential

structural part of the systems and (ii) the superconductivity is primarily supposed to reside in the CuO_2 planes. The superconducting $\text{Bi}(2:2:1:2)$ phase is well suited for a study of the influence of doping elements in the CuO_2 planes, since there is only one position of Cu in the unit cell and the growing of homogeneous single-phase crystals is possible. The other reason for 3d elements to get substituted at the Cu(1), Cu(2) site is due to their closure ionic size and similar outer atomic orbital to that of Cu. Low concentrations of the doping elements Fe increased the pinning force density and shifted the magnetic irreversibility line towards higher fields. Fe create pinning centers in Bi:2212, but it could also increase the grain boundaries resistance, that depressed the critical current densities for high dopant content.

1.11 Bi- base Superconductor

BSCCO was discovered in 1988. BSCCO was the first high temperature superconductor which does not contain any rare earth metals. It is a cuprate superconductor. BSCCO itself can have 1, 2, or 3 CuO planes, with T_c increasing with the number of planes. In the Bi-based system, three phases are observed with the general formula $\text{Bi}_2\text{Sr}_2\text{Ca}_{n-1}\text{Cu}_n\text{O}_{2n+4+\delta}$ where $n=1$ (2201), $n=2$ (2212), $n=3$ (2223) with corresponding superconducting temperatures of 10K, 85K, 110K, respectively.

1.12 Crystal Structure of BSCCO 2212

The high T_c superconductor BSCCO has been studied under X-ray single crystal and neutron diffraction. It has a complex layered perovskite like structure. The crystallographic unit cell of BSCCO contain three layers. They are reservoir layer i.e BiO and SrO that reserves the electron, just above it contains the superconducting layer i.e CuO in this doping is possible to vary the property of superconductors above this it contains the insulating layer (CaO and CuO) where CaO and CuO form the Josephson junction between them. The transition temperature T_c between the superconducting and non-superconducting states is strongly dependent on the concentration of carriers in the CuO_2 planes, which closely relates to structure in charge reservoir and the number of CuO_2 plane. The Bi-2201, Bi-2212 and Bi-2223 phases have single, double and triple layers of CuO_2 in the sub unit cell respectively and more planes are believed to be associated with higher values of T_c ($R=0$). All the three phases have in common both the conduction layer and charge reservoir layer. We prefer to synthesis BSCCO-2212 phase because its T_c is considerably high and it is easy to synthesis as they are thermodynamically stable over a wide range of temperature and within the stoichiometric range, as compared to 2223 phase.

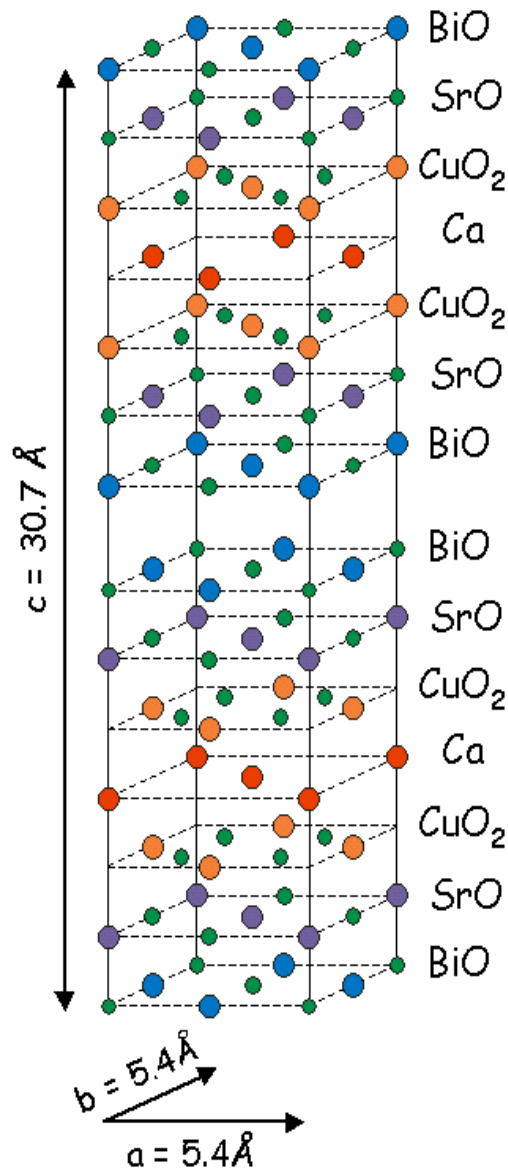


Fig:1.12 Crystal structure of BSCCO

1.10 Literature Survey

For technological reason search has been continued to find a superconducting material which can conduct at room temperature. The first HTSC material LaBaCuO with the T_c of 30K has brought a revolution. And in the subsequent year YBa₂Cu₃O_{7-δ} with T_c of 90K has been discovered. Soon after this a whole host of material has been discovered. Since the common component in all these new high temperature superconductors is a CuO₂ plane, these materials are referred to as the “cuprates.” These materials are anti-ferromagnetic. BSCCO was discovered in 1988. BSCCO itself can have one, two, or three CuO planes, where T_c increases with the number of planes. Although the ceramic method is widely employed for the synthesis of superconducting bismuth cuprates of the type Bi₂ (Ca, Sr)_{n-1}Cu_n

$O_{2n+4+\delta}$, it is generally difficult to obtain mono-phase compositions, due to various factors. Both thermodynamic and kinetic factors are clearly involved in determining the ease of formation as well as phase purity of these cuprates. The $n = 1$ member (2201) of the formula $Bi_2Sr_2CuO_6$ appears to be stable around 1083 K and the $n = 2$ member, $Bi_2(CaSr)_3Cu_2O_8$ (2122) around 1113 K. The $n = 3$ member, $Bi_2(CaSr)_4Cu_3O_{10}$ (2223), can be obtained close to the melting point (1123 K) after heating for several days or even weeks. Among these BSCCO 2212 is the most stable. Bi_2O_3 used as a starting material melts at around 1103K. So increasing the reaction temperature therefore leads to preferential loss of volatile Bi_2O_3 . This results in micro-in-homogeneities and the presence of the unreacted oxides in the final product, so keeping this in mind we have used 5% more than the calculated amount. These materials contain so many cations, partial reaction between various pairs of oxides lead to the formation of impurity phases in the final product which cannot easily be avoided. This can be overcome by employing the matrix reaction method. The matrix reaction method yields mono-phasic $n = 2$ (2122) and $n = 3$ (2223) compositions showing T_c values of 85 K and 110 K respectively. Bismuth can also be replaced with thallium or mercury, which results in the highest T_c material known (153K). BSCCO has been more useful so far in bulk applications; it has been formed into superconducting wires (with silver) and placed into the Detroit. BSCCO-2223 is an extremely anisotropic material, and it is regarded as one of the most technologically significant high T_c phases in the Bi-Sr-Ca-Cu-O system though difficult to prepare in the pure form as it undergoes a change to 2212 (85K) phase. It was observed that the partial substitution of Bi by Pb enhanced the preparation of nearly single phase 2223 material and increase in T_c . The lead (Pb) addition results in the creation of a superconductivity solid solution $Bi_{2-x}Pb_xSr_2Ca_2Cu_3O_8$ by partial substitution of Bismuth (Bi) and the optimum lead content 'x' lies between 0.3 and 0.4. Substitution of lead for bismuth was effective in stabilizing and the formation process of a high T_c phase.

A Sedky et al investigated the structural and transport properties of $La_{1.85}Sr_{0.15}Cu_{1-x}M_xO_y$ ($M = Li, Ni, Co$ and Mn , and $x = 0.00, 0.15$ and 0.30) ceramic samples. They showed that the magnetic doping elements caused lattice deformation resulting in rapid increase in the resistivity more effectively than the nonmagnetic doped samples and lead to the largest change in the transport properties of La 214 systems. They believed that the Mn was not well substituted in the CuO_2 planes of La-214 systems and it might be dissolved in some other sites which had less effect on superconductivity. J. M. Tarascon et. al. reported physical properties resulting from chemical substitution of Cu by Co, Fe, Ni, Al and Zn in the $YBa_2Cu_{3-x}M_xO_{7-y}$ superconductors. They showed that T_c suppression took place with the increasing doping concentration, whether the doping ion is magnetic (Co, Fe, Ni) or diamagnetic (Zn or Al). They

suggested that anisotropic oxide structure of these compounds made them different, in behaving with respect to magnetic impurities, from conventional BCS-type superconductors.

M. A. K. L. Dissanayake et al.¹³⁸ reported the superconducting properties of a series of compounds of nominal composition $(\text{Bi}_{0.7}\text{Pb}_{0.3})\text{SrCa}(\text{Cu}_{1.5-x}\text{Ni}_x)\text{O}_\delta$ ($x=0-1.1$). Up to $x = 0.2$ composition, T_c drops down to 60 K rather fast. From $x = 0.2$ to 0.95 the material remains superconducting with T_c around 50K. For $x \geq 1.0$, the material becomes semi-conducting. N.K. Man et al proposed that the decrease of T_c with increasing Ni content was mainly due to distortion of the crystal structure by the extra oxygen intercalated between two adjacent BiO layers which then affected the hole concentration of the copper planes. Additionally, the decrease of T_c was suggested to be due to the impurity Ni substituted for the Cu in the CuO_2 planes. The effect of magnetic and nonmagnetic impurities (Ni, Zn)

substitution for Cu in $\text{Bi}_2(\text{SrCa})_{2+n}(\text{Cu}_{1-x}\text{M}_x)_{1+n}\text{O}_y$ whiskers was studied by Y. K. Kuo et al. These whisker crystals showed resistance drops for both the 2212 and 2223 ($n=1, 2$) phases, with transition widths (10–90 %) of 1 K. They observed a linear depression of T_c for both 2212 and 2223 phases with $D = dT_c/dx = -800$ K for both Ni and Zn. G. Ilonca et.al. reported that doping with Ni and Fe could create pinning centers in Bi:2212, but it could also increase the grain boundaries resistance, that depressed the critical current densities for high dopant content. They concluded that a pair-breaking scattering process induced by the dopants was responsible for the initial suppression of the T_c . They thought that the most probable pair-breaking scattering process was a scattering on paramagnetic, local Cu spins induced close to the doping elements. On the other hand, the effects of Zn and Ni doping in the electron-doped systems appeared to be opposite from the hole doped case, i.e., Ni impurities lead to a stronger suppression of the superconducting ordering temperature than Zn doping. Low concentrations of the doping elements, typically below 1 at.%, definitely increase the pinning force density while higher concentrations strongly suppressed the critical current density.

So from the literature survey we conclude that Bi-2212 also has lower current densities due to weak link problem, so for making it for practical application their properties can be enhanced by doping with transition metal. By doping with transition metal it creates pinning centers which pin the vortex motion and hence it increases its current density in high magnetic field.

Objective

- ✓ To synthesis BSCCO 2212 phase.
- ✓ Doping with Fe in BSCCO 2212 for 1%,3%,5%.
- ✓ To study the effect of doping and how it helps to increase the current density.

Chapter- 2

Experimental method and Characterization techniques

2.1 Sample Preparation

Many methods have been developed in order to develop superconducting oxide. Synthesis of sample in single phase is the most important. Various methods have been developed to prepare BSCCO-2212. These are solid-state synthesis route, chemical precipitation, melt process, spray pyrolysis, sol-gel synthesis route, etc. We prefer solid-state reaction because it gives homogeneous product. In solid-state reaction the expected phase is the consequence of five elements diffusion and is the result of reaction between several precursors phases. That is why many grindings and long calcinations at high temperatures is required to obtain single phase powder. Precursors oxide powders are palletized and then sintered (heat treatment below the melting temperature) to get high T_c phase.

(a) Materials Used

Samples of Bi-based superconductors were prepared using 99.99% pure powders of Bi_2O_3 , CaCO_3 , Sr_2O_3 and CuO as a starting material. Samples were accurately measured in the stoichiometric ratio for 2212 phase.

(b) Agate Mortar and pestle

After mixing of powders it was grinded in the Agate mortar and pestle. During heat treatments intermediate grindings are necessary for uniformity and to reduce the particle size. Agate mortar and pestle are used to grind solid into fine powders but under conditions that are highly controlled and to minimize the contamination.

(c) Hydraulic Press

Pellets of the calcined powders were made before sintering. The compactness of the pellet depends on the size of the particles, pressure applied and duration. Pressure of 5 Kg/cm^2 has been applied to pelletized.

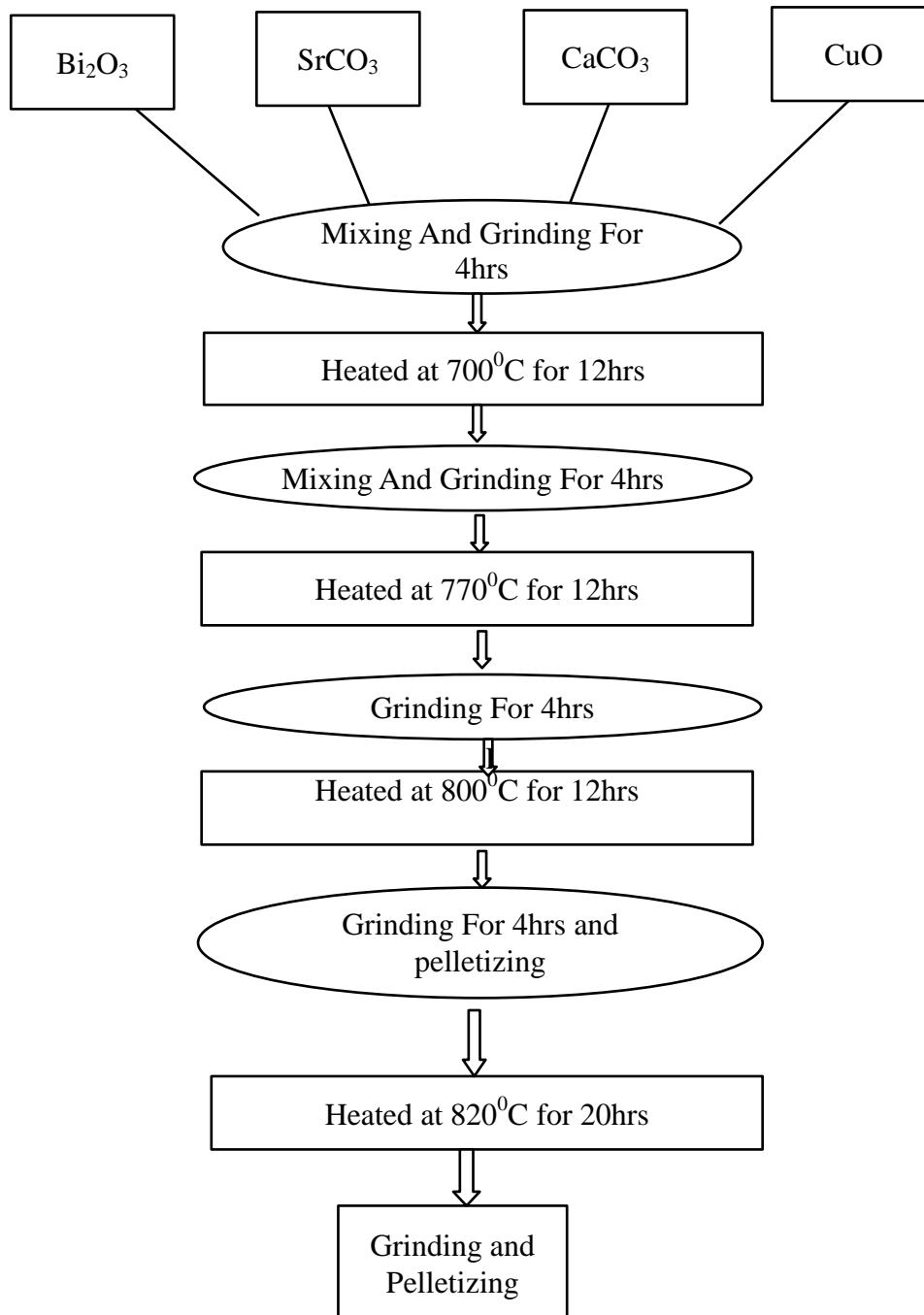
(d) High temperature furnace

In order to carry out heat treatments i.e. calcinations, sintering high temperature electric furnace was used. Furnace was equipped with programmable controller having maximum temperature up to 1300°C .

(e) Steps for preparation

1. Here the precursors powder CaCO_3 , Bi_2O_3 , Sr_2O_3 and CuO with 99% purity as starting material are taken. These are mixed in appropriate amount with a Bi:Sr:Ca:Cucation ratio of 2:2:1:2 and finally grinded with mortar-pestle for 3 hrs and the resultant mixture was calcined in electric furnace for 12 hrs at 700°C .
2. The sample is allowed to cool naturally and it is again grinded for 3 hrs with motar pestal and calcined in electric furnace for 12 hrs at 770°C .
3. The grinding process is repeated and the sample is calcined for 20 hrs at 820°C for 20 hrs.
4. Finally the sample is pressed into pellet of 10mm diameter and 5mm thickness by dry pressing method and sintered at 880°C for 12 hrs.

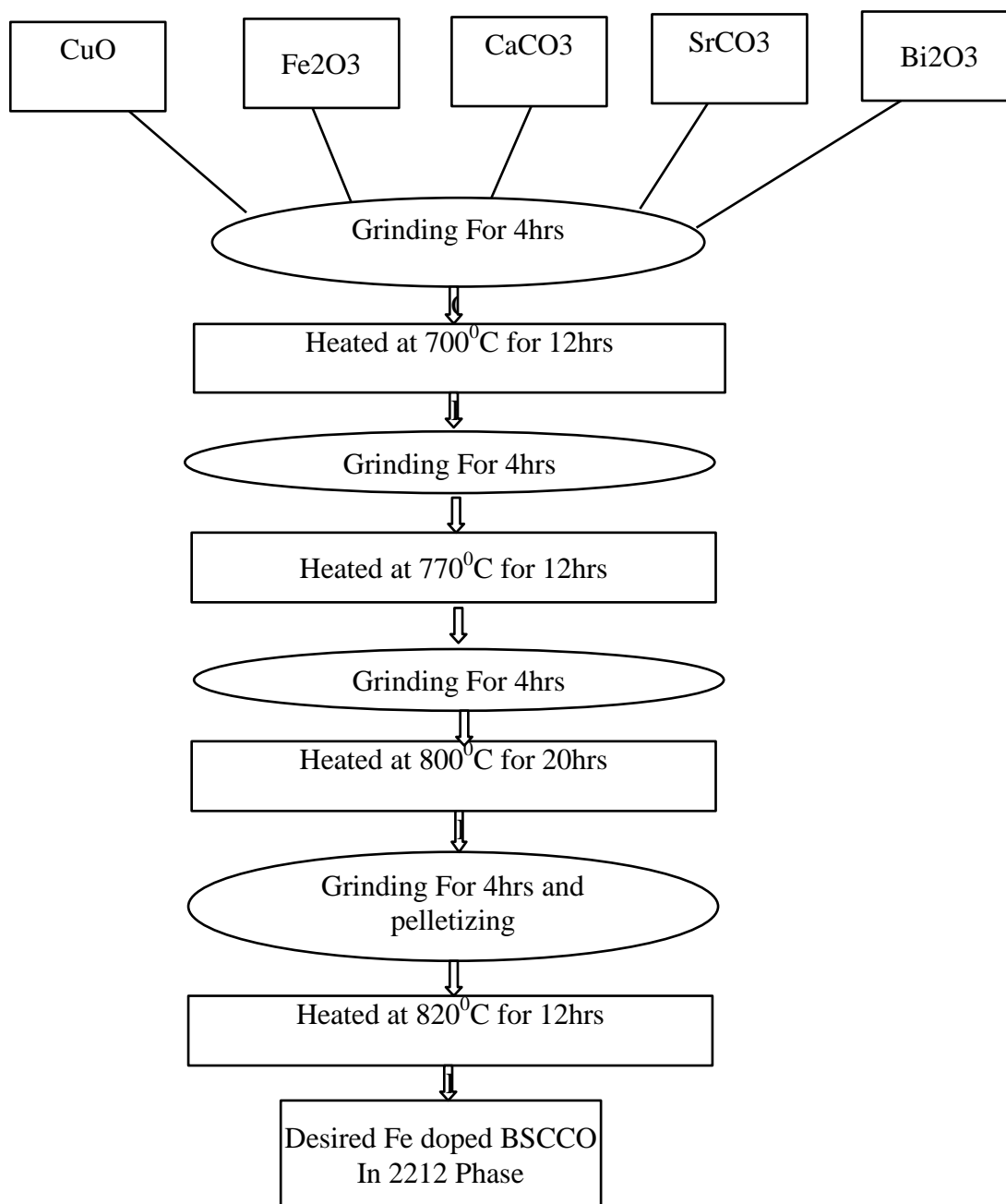
FLOW CHART FOR BSCCO SYNTHESIS



2.2 Synthesis of Fe doped BSCCO with different concentration

Fe is doped in BSCCO 2212 in Cu site for this calculation is done for 1%,3%,5% concentration of Fe in BSCCO. And same procedure is followed as that of BSCCO.

FLOW CHART FOR Fe doped BSCCO SYNTHESIS



2.3 Characterisation Techniques

The sample has been characterised using different techniques to study its properties. Here we have done XRD, SEM. R-T measurement has also been done which give the critical temperature and critical current density.

2.3.1 XRD

X-ray diffraction is a characterization tool that can be used to determine different material properties including crystal structure, grain orientation, changes in lattice parameters or distinguishing between phases in a multi-phase material.

It works on Bragg's law which state that

$$2d\sin\theta = n\lambda$$

According to this law X-rays with a single wavelength (λ), a relationship exists between the spacing of atomic planes (d_{hkl}) and the angle (θ) at which diffracted x-rays will constructively interfere with each other. Where the wavelength (λ) of X-ray is comparable to the interplaner spacing (d) of the crystal. In X-ray diffraction work we normally distinguish between single crystal and polycrystalline or powder applications. A simple way to understand how this law helps to characterize materials is to realize that different crystalline materials have different planar spacing, therefore diffraction will constructively interfere at different angles depending on the material. If this interference is plotted against twice the angle, then the location of the constructive peak will change depending on what material is being examined. Now within a three dimensional crystal, many planes of atoms exist, so one material will have many peaks, but all located at an angle specific to the distance between those planes. This plot is known as an x-ray diffraction pattern and can be used to identify materials. Measurements were done at room temperature since there is no change in the superconducting materials before and after transition. XRD data was used to identify different phases present in the samples and lattice parameters.

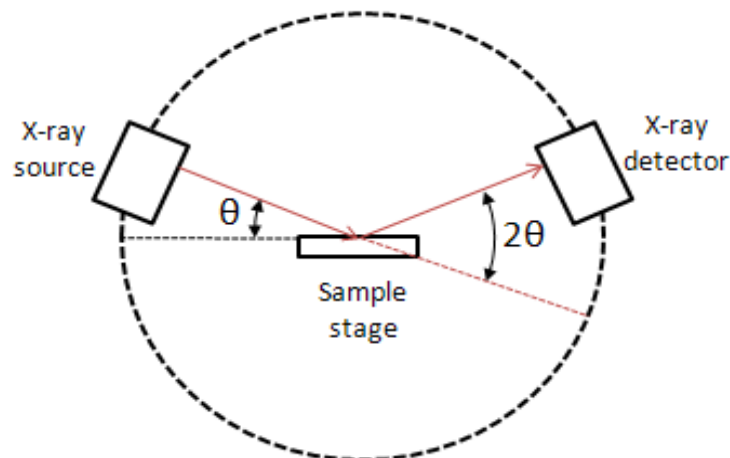


Fig:2.3.1 Systematic XRD system

2.3.2 Scanning Electron Microscope

The scanning electron microscope (SEM) is widely used in the analysis of a specimen's microstructure and phase composition. It enables the investigation of specimens with a resolution down to the nanometer scale. An SEM works by bombarding a specimen with a finely focused electron beam that scans across its surface. This beam interacts with a region at the sample surface and produces secondary electrons, backscattered electrons, auger electrons, and also characteristic x-rays. A different detector is used for each emission, depending on what type of information is needed.

Secondary electrons have relatively low energies (~ 10 eV) and are emitted from a volume close to the surface, near the beam impact area. These electrons carry information regarding the specimen's surface topography. Backscattered electrons carry higher energies (5 – 40 keV) and penetrate the specimen farther than secondary electrons. Backscattered electrons transmit information on the specimen's chemical composition, crystal orientation, and due to an interaction with secondary electrons, surface topography as well. We have been using the conventional scanning electron microscope, which operates in high vacuum, and the specimen has to be electrically conductive or has to be coated with a conductive layer (e.g. Carbon, Gold etc.).



Fig:2.3.2 Scanning Electron Microscope

2.3.3 R-T Measurement

Resistivity is the opposition offered to the flow of current. At constant temperature the resistance R , of a conductor (i) is proportional to the length (ii) inversely proportional to its area of cross section.

$$R \propto L/A$$

or, $R = \rho L/A$

The constant of proportionality ρ is called resistivity of the material of the conductor.

Resistivity of the material is equal to the resistance offered by a wire of this material of unit length and unit cross-sectional area. Unit of resistivity is ohm-meter ($\Omega \cdot m$)

Two Probe Method

For a long thin wire like geometry of uniform cross-section the resistivity ρ can be measured by measuring the voltage drop across the sample due to the passage of known current through the sample.

The potential difference between the two contacts is measured by voltmeter. Let the current in the sample is I , it is measured by Ammeter. Let l be the length of the sample between two probes and A be the cross-sectional area, then the resistivity of the specimen is

$$\rho = VA/Il$$

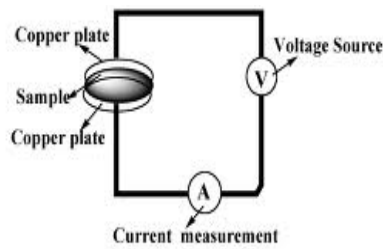


Figure 3: The set-up for two-probe conductivity measurement

The major drawback of this method is the error due to contact resistance of measuring leads $V=(2r+R)I$. The method can also be not used for materials having random shape.

Four Probe Method

To overcome the above problem Four Probe method has been introduced. In this resistivity of the specimen having wide variety of shape can be but uniform cross-section can be measured. The four probe set up consists of four equally spaced tungsten metal tips with finite radius. Current source is used to supply current through the outer two probes, a voltmeter measures the voltage across the inner two probes to determine the sample resistivity. The inner probes draw no current because of the high input impedance voltmeter in the circuit.

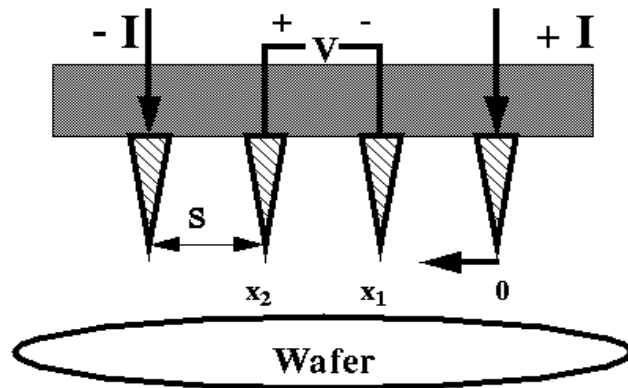
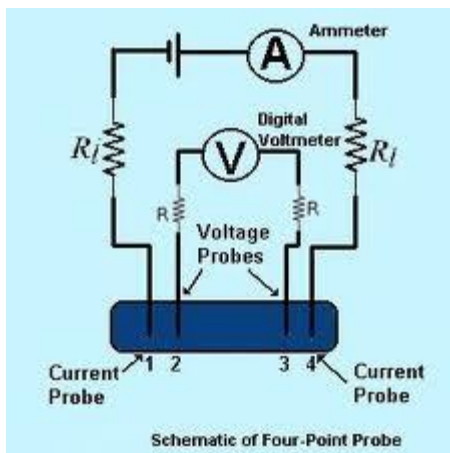


Fig:2.3.3(a) Four Probe measurement technique

The Van der Pauw method

This technique is used when the geometry of the sample is not known. This technique was developed in order to measure the resistivity of the thin and flat samples of semiconductors but this is also applied to the case of superconductors.

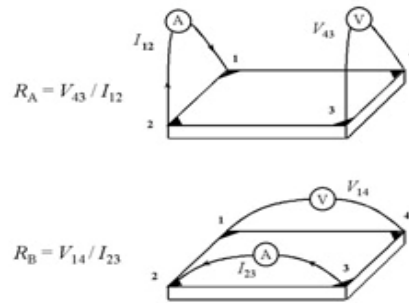


Figure 2

Fig:2.3.3(b) Van der pauw method

Low resistance samples are difficult to measure using an ohmmeter. Using the ohmmeter setting on a multimeter means that you will measure the resistance of the sample plus the connecting leads to the sample. Standard four probe technique was used for electrical characterization of superconducting samples. Silver conducting paste was used to make the contacts on the sample, the contact resistance being in the order of 0.1Ω or lower.

CHAPTER- 3

RESULT AND DISCUSSION

3.1 XRD ANALYSIS

The XRD powder pattern for the samples was done at room temperature. The sample was scanned in a continuous mode from 20° - 80° with the scanning rate of $3^{\circ}/\text{min}$. The XRD pattern of parent BSCCO sintered at 880°C for 12 hrs and 1%, 3% and 5% Fe doped BSCCO are shown in the given Fig3.1. The XRD pattern of BSCCO has sharp well defined peaks. The indexed peaks correspond to the 2212 phase. On doping with 1%, 3% and 5% Fe the structure of BSCCO does not change and the major peaks still correspond to 2212 phase. The value of lattice constants were calculated from the reflection corresponding to BSCCO T_c phase and found to be ($a = 3.82\text{\AA}$, $b = 3.82\text{\AA}$ & $c = 30.60\text{\AA}$) which clearly suggests the tetragonal structure.

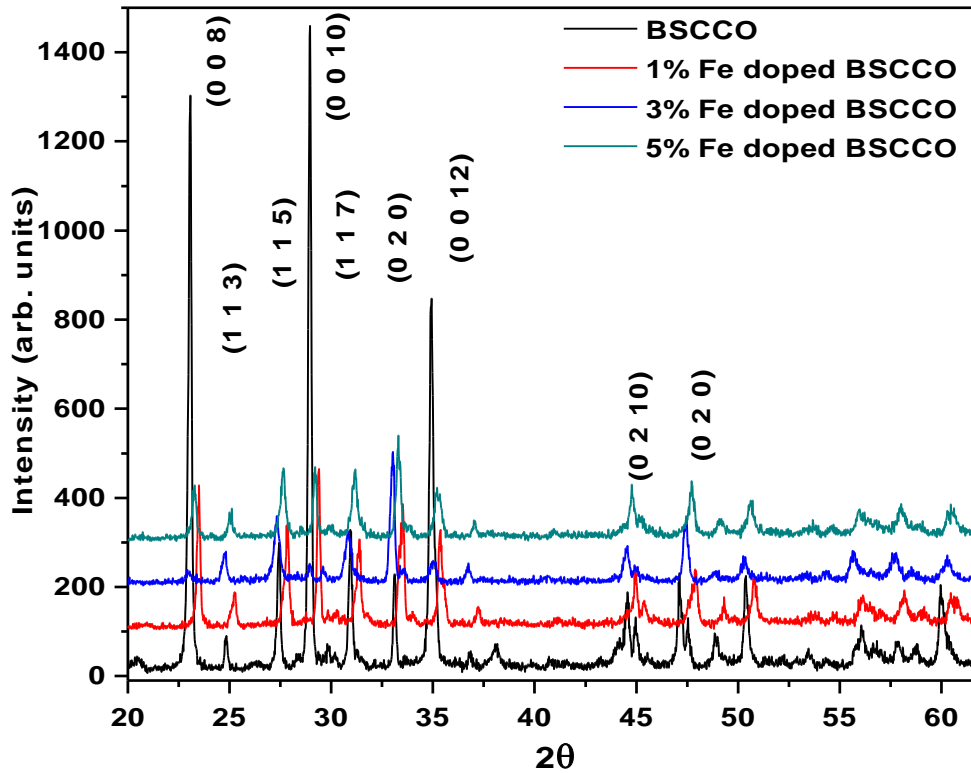


Fig:3.1 X-Ray Diffraction Pattern of BSCCO, 1%, 3% & 5% Fe doped

3.2 SEM ANALYSIS

SEM is an useful tool to probe the microstructure of superconductors, as the phenomenon of superconductivity initially develops within the grain and eventually crosses over the grain boundaries, leading to the bulk. From the SEM micrograph the flake type of grains with some needle shape grain are seen. These needle shape grains have size ranging from $1.03 - 8.95\mu\text{m}$. Further analysis of these needles indicates that they are poor in bismuth[22]. The grains are oriented randomly with no particular direction showing anisotropic nature of BSCCO. With the addition of Fe the grain size decreases. This may be due to the increase of strain leading the particles break into smaller sizes. Also, the Fe-doped samples show more number of voids and poor connectivity of grains. Thus grain connectivity becomes more important for the sharpness of transition and other critical parameters.

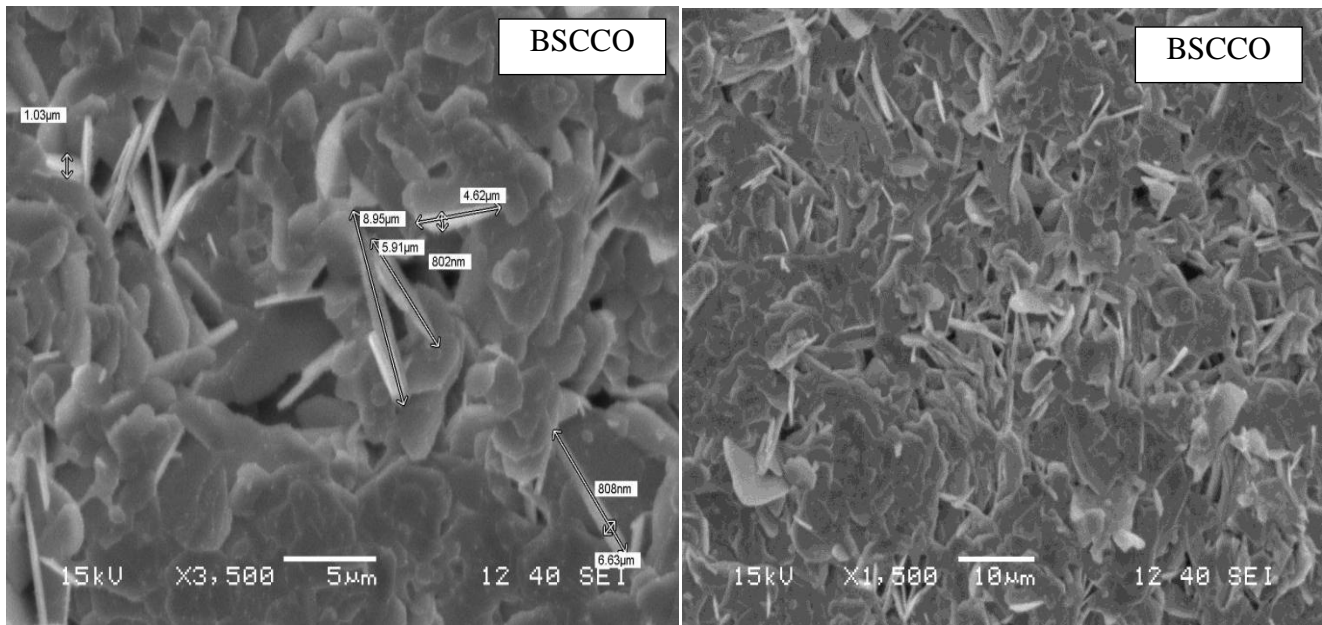


Fig:3.2(a) SEM Micrographs Of BSCCO

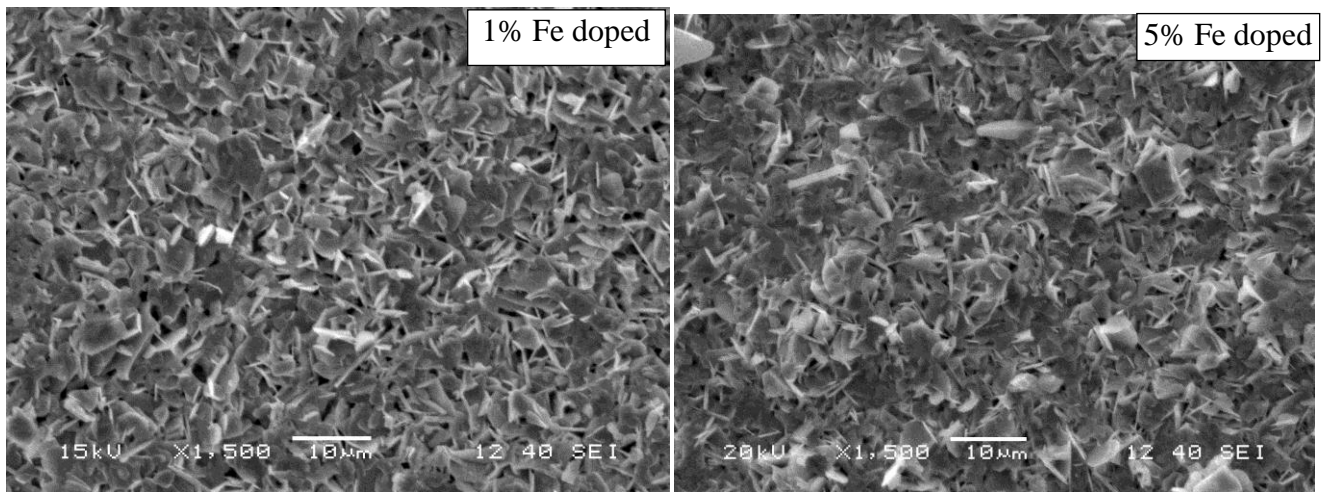


Fig:3.2(b) SEM micrographs of 1% and 5% Fe doped in BSCCO 2212

3.3 Resistivity vs Temperature Analysis

Temperature dependence of resistivity is a well known technique to know the variation of resistance with temperature and to determine at which temperature its resistivity becomes zero. Standard four probe technique was used for electrical characterization of superconducting samples. Sample was mounted on the cryocooler setup and silver conducting paste was used to make the contacts on the sample. Resistivity measurements were carried out from 300K to 6K by four probe configuration with $1 \mu\text{V}/\text{cm}$ used as criterion for J_c measurement. Janis Cryostat equipped with rotary pump and temperature controller (Lake Shore-331) was used for monitoring and controlling temperature down to 6K temperature. A constant current of 10 mA was passed through the samples, with the help of constant current source (Keithley Model-2161) and voltage drop measured by nano-voltmeter (Keithley Model-2182). The electrical resistivity verses temperature curve for all the samples (BSCCO, 1%Fe doped, 3% Fe doped, 5% Fe doped) were measured from 300K to 8K. The resistivity is normalized w.r.t 273K, ρ/ρ_{273} , the graphs are shown in the Fig.3.3(a) from the graph we can see that the graph is linear above T_c -onset indicating the metallic behaviour above T_c -onset. T_c onset for different samples BSCCO, 1% Fe doped, 3% Fe and 5% Fe doped are 88.84K, 72.00K, 68.57K and 66.60K respectively. At T_c -onset graph shows a sharp decrease it is the temperature at which material enter from metallic to superconducting state and it becomes completely superconducting at T_{c0} where resistance becomes zero. By finding the first order derivative dR/dT and plotting a graph between dR/dT Vs T we can find T_c i.e mean field transition temperature at which the phase change takes place from metallic to

superconducting phase. Different T_c obtained for BSCCO, 1%, 3% and 5% Fe doped are shown in the graph of Fig:3.3(b) these are 78.31K, 60.80K, 59.09K, 52.72K. The transition shifts continuously towards lower temperatures with increasing dopant concentration. For 3% Fe we can see higher T_c -onset this may be due to the weak link transition become smoother with strong link a similar trend has been observed by “L Ponta et.al [21], but it has not been explained. The lower T_c may be due to the strain induced when the samples are mechanically deformed[23]. Fe-doped samples with concentrations of 1% 3% and 5% of Fe the transition is strongly broadened, indicating an inhomogeneous distribution and clustering of the Fe atoms at the grain boundaries or we can say due to the poor inter-grain connectivity. There is nearly zero residual resistance indicating a high degree of perfection in crystalline solid.

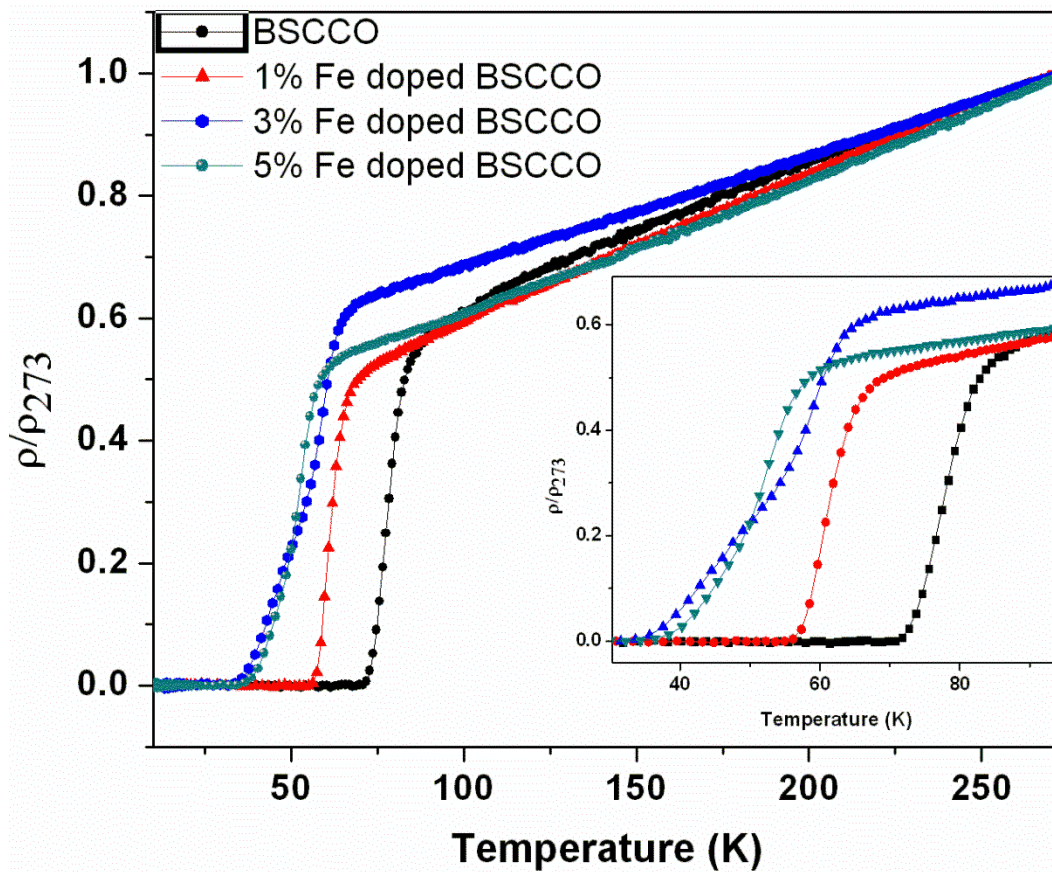


Fig:3.3(a) Temperature variation of normalized resistivity ρ/ρ_{273} for BSCCO and 1%, 3%, 5% Fe doped

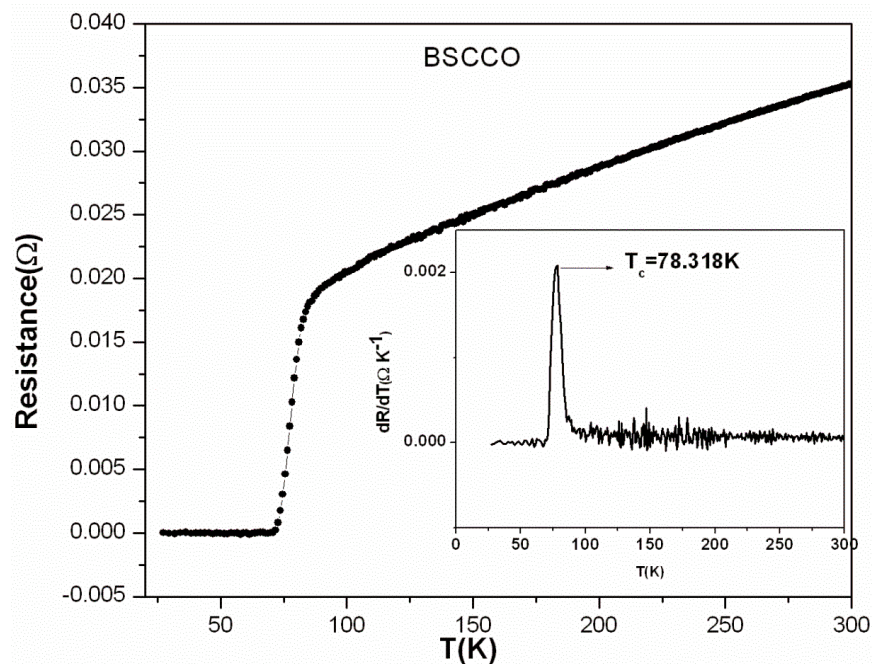


Fig:3.3(b) Resistivity(R) versus temperature(T) for BSCCO is shown. The inset is the plot of dR/dT versus Temperature .

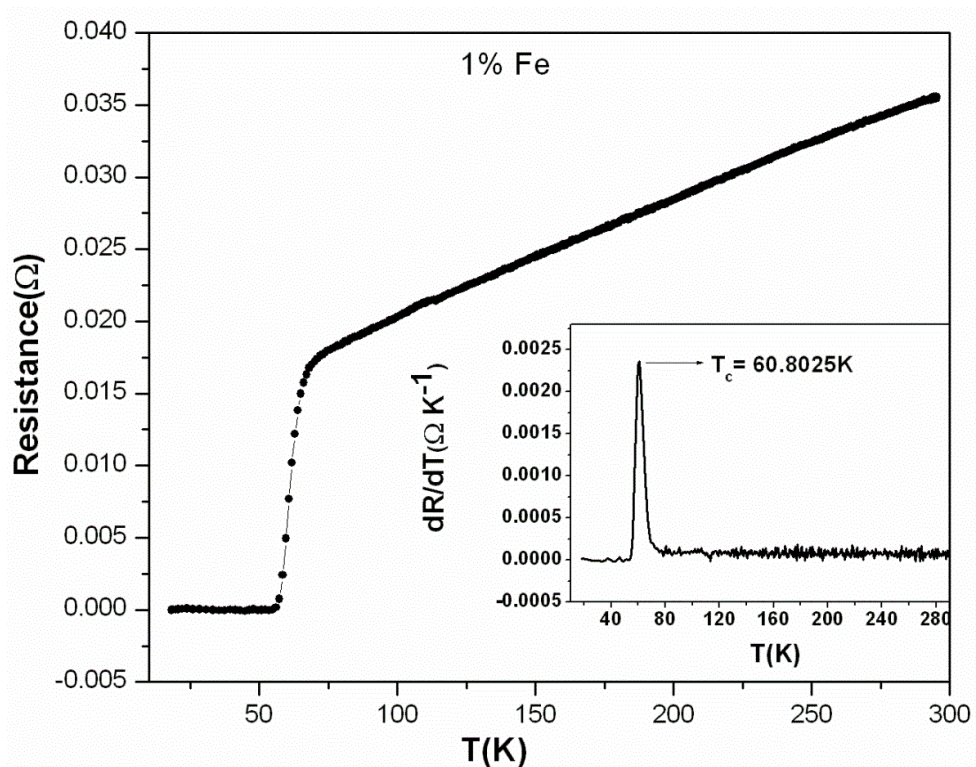


Fig:3.3(b) Resistivity(R) versus temperature(T) for 1% Fe doped BSCCO is shown. The inset is the plot of dR/dT versus Temperature.

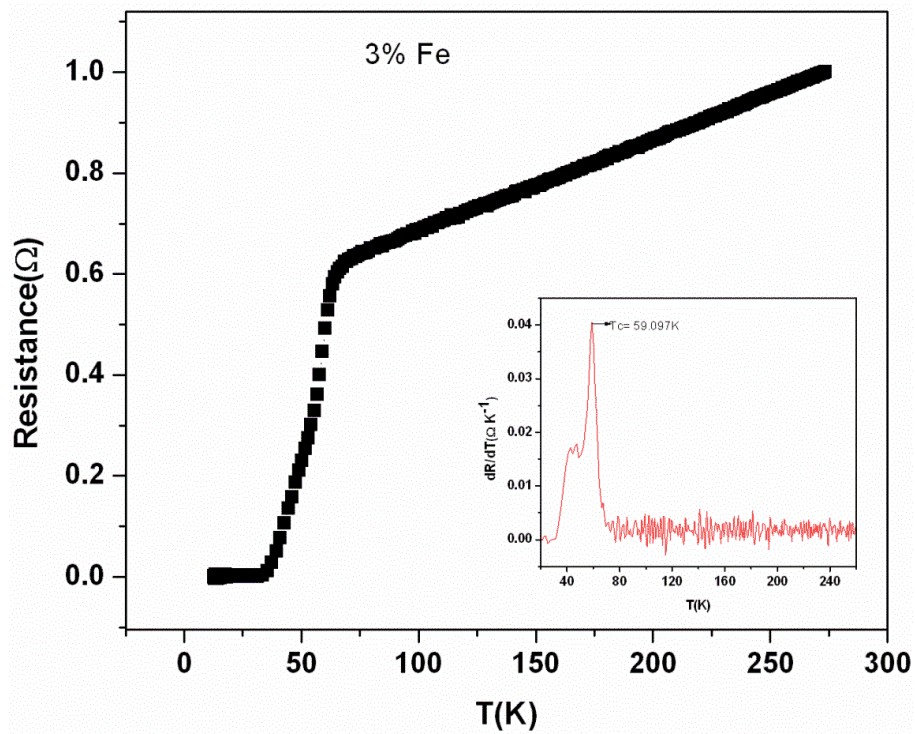


Fig:3.3(b) Resistivity(R) versus temperature(T) for 3% Fe doped BSCCO is shown. The inset is the plot of dR/dT versus Temperature.

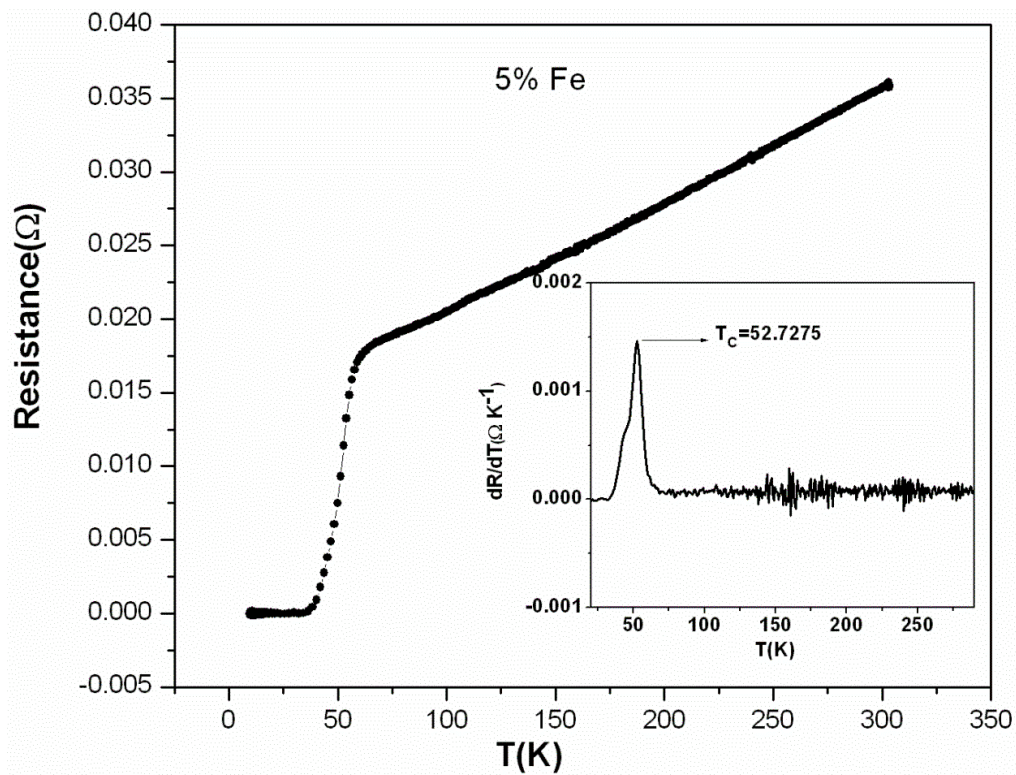


Fig:3.3(b) Resistivity(R) versus temperature(T) for 5% Fe doped BSCCO is shown. The inset is the plot of dR/dT versus Temperature.

3.4 Current Density

Critical current density versus temperature graph has been plotted which show that J_c increases with decrease of temperature. J_c has been calculated as $J_c = I_c/A$ where A is the cross sectional area of the sample and I_c is the critical current density. The critical current density is obtained from V-I curves at a fixed temperature. Taking Josephson junction into consideration, when the temperature decreases to critical temperature T_c , almost all the grains become superconducting together with the parts of the non-superconducting. With the equation $J_c(T) = J_c(0)(1-T/T_c)^n$ we can calculate the value of “n” by fitting the curve for $J_c(T)$ verses T . Depending on the value of we can detect the type of Josephson junction i.e for $n=1$ it is superconductor-insulator-superconductor and for $n=2$ it is superconductor-normal metal-superconductor. The value of n is calculated by fitting of the equation $J_c(T) = J_c(0)(1-T/T_c)^n$ n value increases by doping with Fe indicating superconductor-insulator-superconductor behavior of the junction as Fe is doped. And the value of current density is maximum for 5% Fe doped.

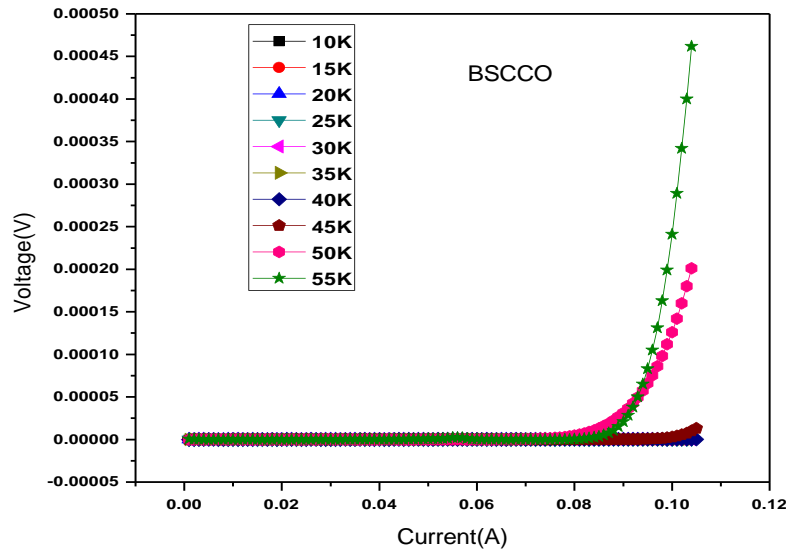
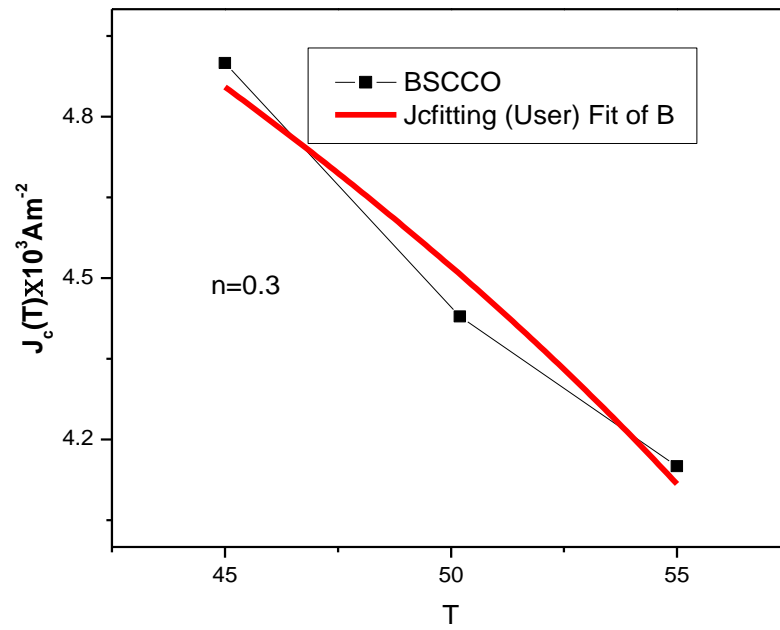


Fig:3.4(a) V-I characteristic of parent BSCCO



Variation of critical current density J_c as a function of temperature

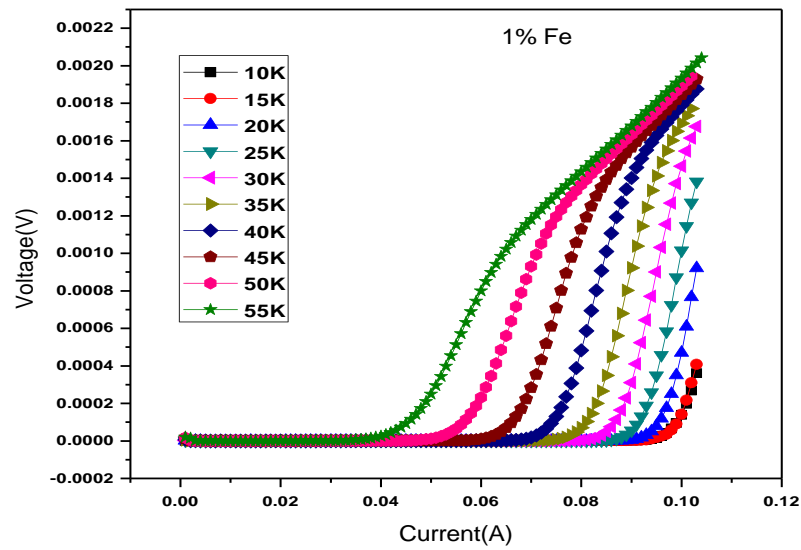


Fig:3.4(b) V-I characteristic of 1% Fe

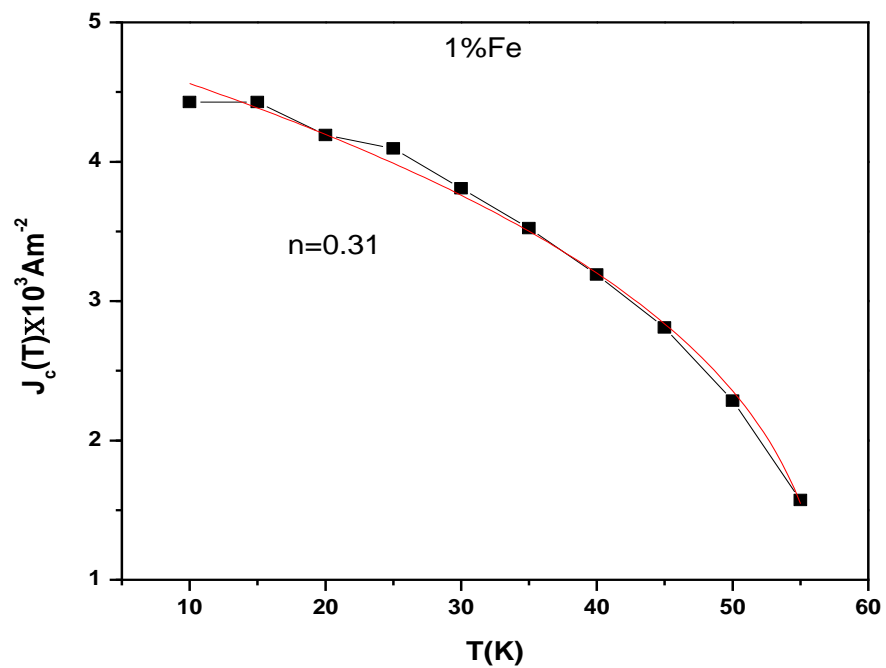


Fig:3.4(b) Variation of critical current density J_c as a function of temperature

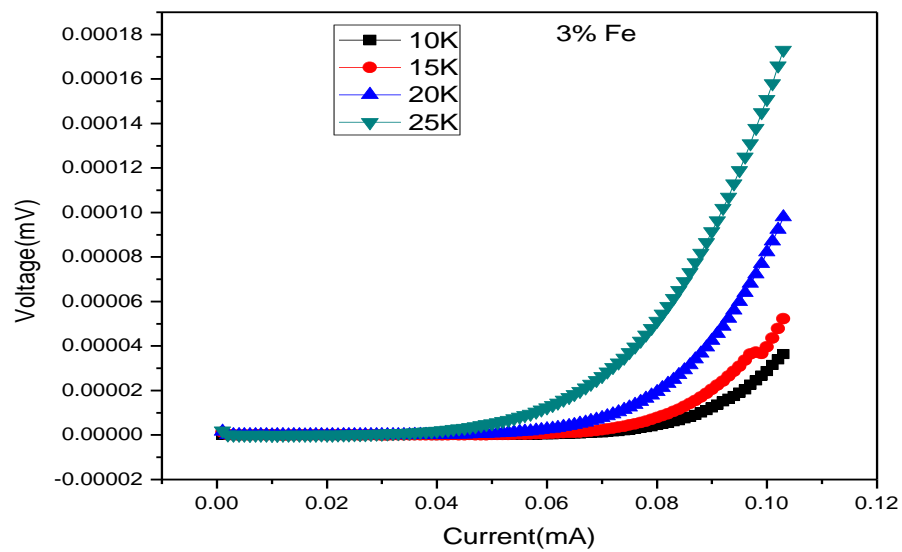


Fig:3.4(c) V-I characteristic of 3% Fe

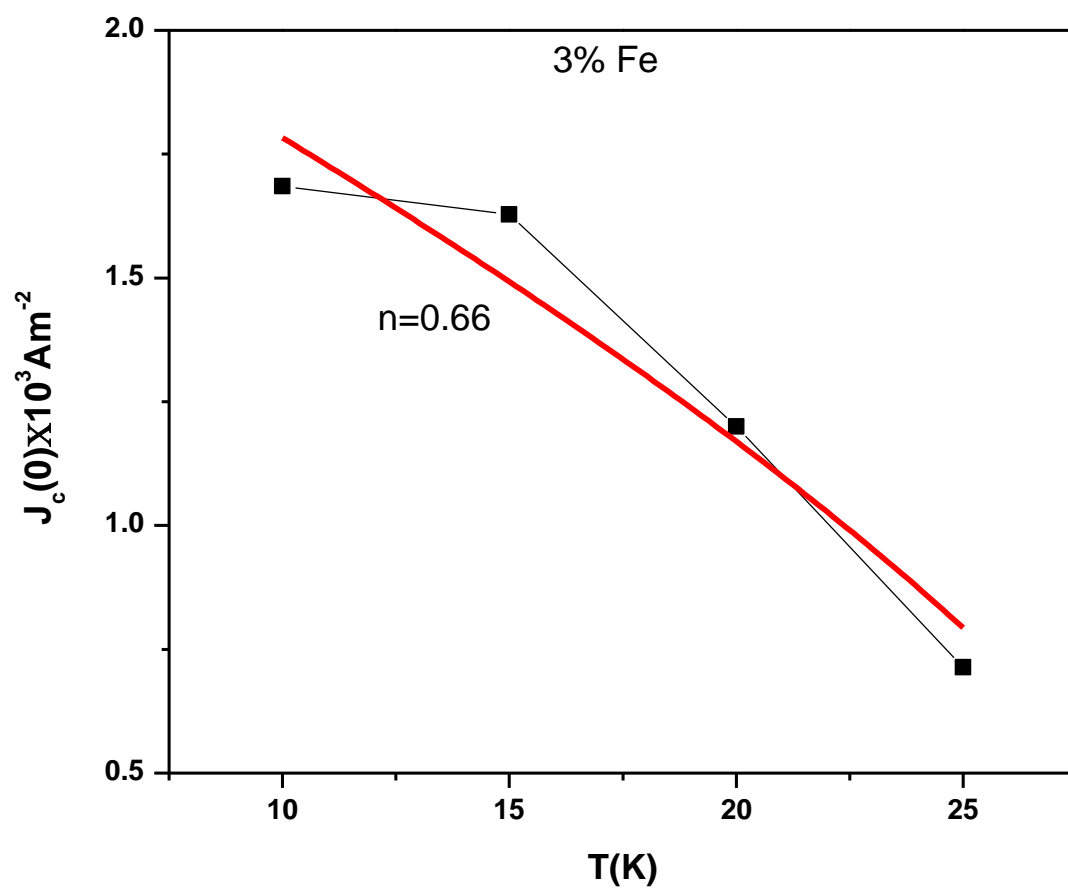


Fig:3.4(c) Variation of critical current density J_c as a function of temperature

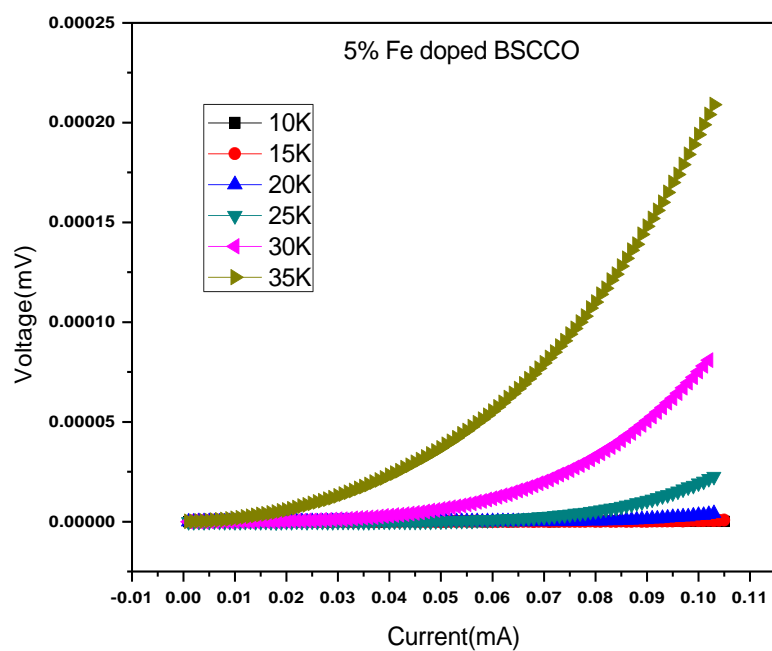


Fig:3.4(d) V-I characteristic of 5% Fe

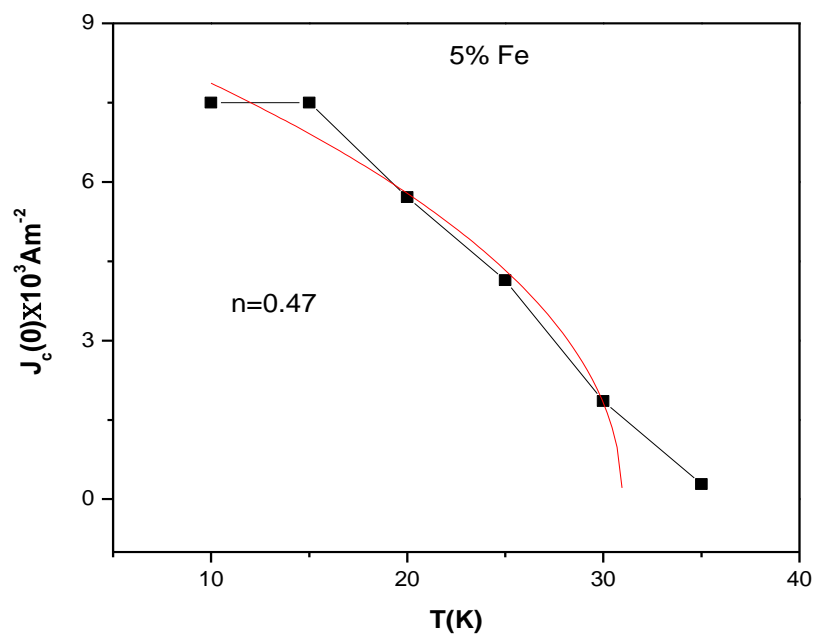


Fig:3.4(d) Variation of critical current density J_c as a function of temperature

3.5 Jc Verses Concentration

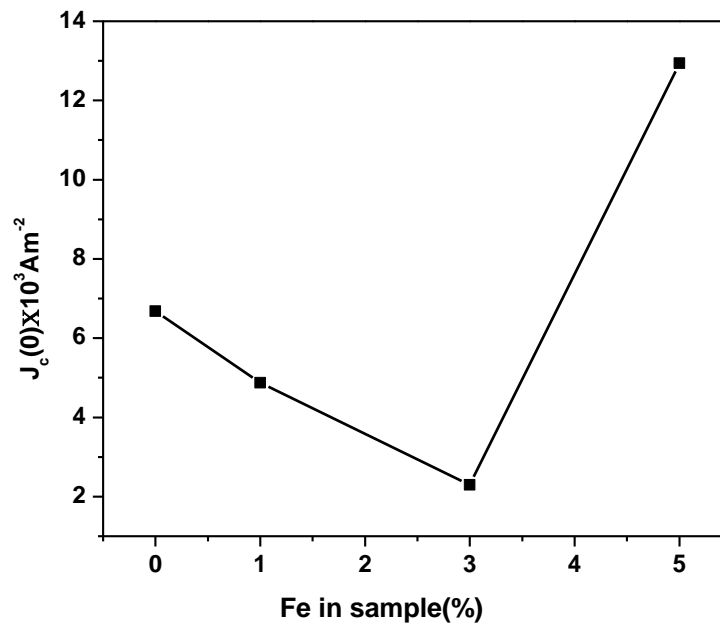


Fig:3.5 Variation of J_c with different concentration of Fe doped in BSCCO

From the graph it is clear that J_c decreases for initial concentration of Fe and is maximum for 5% Fe doped. Hence Fe acts as a strong pinning centre.

Fe Con.	$J_c(\text{mA/m}^2)$	n
0% (BSCCO)	6.68	0.3
1%	4.87	0.31
3%	2.30	0.66
5%	12.94	0.98

Chapter 4

Conclusion:

The sample BSCCO with 2212 phase and its doping with different concentration of Fe(1%, 3%, 5%) has been prepared successfully by solid state synthesis route. The sample was characterized by xrd which shows sharp peaks corresponding to BSCCO 2212. And with doping there is no any additional phase has been seen which shows that there is no any structural change takes place.

From SEM picture, parent BSCCO with flaky and needle like structure has been observed. The grain size decreases with the addition of Fe in different concentration, which acts as a pinning centre and increases the critical current density.

From Resistivity Vs Temperature graph T_c for BSCCO is found to be 78.32K, found from derivative of dR/dT where there is a sharp peak. As doping is done with different concentration of Fe a gradual decrease in T_c is observed. A broadening in the transition is observed this is due to the poor inter-grain connectivity.

References:

- [1] Charles Kittel, *Introduction to solid state physics*, Seventh edition, Wiley India, 2004
- [2] <http://www.wordiq.com/definition/Superconductivity>
- [3] M Ali Omar, *Elementary Solid State Physics*.
- [4] High Temperature Superconductor www.wikipedia.com
- [6] T. Silver et.al, Developments in high temperature superconductivity, University of Wollongong, Online Annu. Rep. Prog. Chem., Sect. C, **98**, 323–373 (2002).
- [7] H. Q. Li et.al, High temperature superconducting Josephson junctions in a stacked bicrystal geometry.
- [8] G. Blumberg, Evolution of Magnetic and Superconducting Fluctuations with Doping of High- T_c Superconductors
- [9] RH Patel et.al, Characterization of superconducting properties of BSCCO powder prepared by

attrition milling, Supercond. Sci. Technol. **18** 317–324 (2005).

[10] Masatsugu Suzuki et.al, Lecture Note on Solid State Physics Ginzburg-Landau Theory for Superconductivity, January 16, 2007 Department of Physics, State University of New York at Binghamton

[11] Y.Sun et.al, Anomalous Tail effect on Resisitivity Transition and Weak-link Behaviour of Iron Based Superconductor, Physics, Chinese Academy of Sciences, Beijing 100190, P.R.China

[12] BSCCO www.wikipedia.com

[13] Hellstrom E E 1995 Processing Bi-based high-Tc superconducting tapes, wires, and thick films for conductor applications High-Temperature Superconducting Materials Science and Eng, NATURE, **414**, 368-377 (2001)

[14] German R M 1984 Powder Metallurgy Science (Princeton, NJ: Metal Powder Industries Federation) p 62

[15] Kim C-J, Park H-W, Kim K-B and Hong, Supercond. Sci. Technol. **8**, 652 (1995).

[16] Yavuz M, Maeda H, Vance L, Liu H K and Dou S X 1998 Supercond. Sci. Technol. **11** 1153

[17] H. Kamerlingh Onnes, *Nobel lecture by H.K. Onnes, December 11, 1913*
http://nobelprize.org/nobel_prizes/physics/laureates/1913/onnes-lecture.html

[18] M.K. Wu, J.R. Ashburn, C.J. Torng, P.H. Hor, R.L. Meng, L. Gao, Z.J. Huang, Y.Q. Wang, and C.W. Chu, *Phys. Rev. Lett.* **58**, 908 (1987)

[19] <http://www.cartage.org.lb/en/themes/sciences/physics/SolidStatePhysics/Superconductivity/Fundamentals>

[20] W. Lang, G. Heine, Phys. Rev. B **51**, 9180 (1995).

[21] L Ponta, supercond.Sci., Technol. **24**, 015006(11pp) (2011).

[22] M.A.Subramanian et.al “A New High Temperature Superconductor: Ba₂Sr_{3-x}CaxCu₂O_{8+y}” Central Research and Development, E.I. du Pont de Nemours and Company)

[23] K Yamamoto et.al Mechanical and superconducting properties of PIT-processed MgB₂ wire after heat treatment Supercond. Sci. Technol. **16**, 1052–1058 (2003)

*****-----*****